arXiv:cond-mat/0306670v2 [cond-mat.str-el] 13 Dec 2003

Kondo effect in systems with dynamical symmetries

T. Kuzmenko[1], K. Kikoin[1] and Y. Avishai[1,2]
[1]*Department of Physics and* [2]*Ilse Katz Center, Ben-Gurion University, Beer-Sheva, Israel*
(Dated: February 2, 2008)

This paper is devoted to a systematic exposure of the Kondo physics in quantum dots for which the low energy spin excitations consist of a few different spin multiplets $|S_iM_i\rangle$. Under certain conditions (to be explained below) some of the lowest energy levels E_{S_i} are nearly degenerate. The dot in its ground state cannot then be regarded as a simple quantum top in the sense that beside its spin operator other dot (vector) operators $\mathbf{R}_n$ are needed (in order to fully determine its quantum states), which have non-zero matrix elements between states of different spin multiplets $\langle S_iM_i|\mathbf{R}_n|S_jM_j\rangle \neq 0$. These "Runge-Lenz" operators do not appear in the isolated dot-Hamiltonian (so in some sense they are "hidden"). Yet, they are exposed when tunneling between dot and leads is switched on. The effective spin Hamiltonian which couples the metallic electron spin $\mathbf{s}$ with the operators of the dot then contains new exchange terms, $J_n\mathbf{s}\cdot\mathbf{R}_n$ beside the ubiquitous ones $J_i\mathbf{s}\cdot\mathbf{S}_i$. The operators $\mathbf{S}_i$ and $\mathbf{R}_n$ generate a dynamical group (usually $SO(n)$). Remarkably, the value of n can be controlled by gate voltages, indicating that abstract concepts such as dynamical symmetry groups are experimentally realizable. Moreover, when an external magnetic field is applied then, under favorable circumstances, the exchange interaction involves solely the Runge-Lenz operators $\mathbf{R}_n$ and the corresponding dynamical symmetry group is $SU(n)$. For example, the celebrated group $SU(3)$ is realized in triple quantum dot with four electrons.

PACS numbers: 72.10.-d, 72.15.-v, 73.63.-b

I. INTRODUCTION

Recently, studies of the physical properties of artificially fabricated nano-objects turn out to be a rapidly developing branch of fundamental and applied physics. Progress in these fields is stimulated both by the achievements of nanotechnology and by the ambitious projects of information processing, data storage, molecular electronics and spintronics. The corresponding technological evolution enabled the fabrication of various low-dimensional systems from semiconductor heterostructures to quantum wires and constrictions, quantum dots (QD), molecular bridges and artificial structures with large molecules built in electric circuits[1]. This impressive experimental progress led to the development of nanophysics, a new aspect and research direction in quantum physics[2]. Artificial nano-objects possess the familiar features of quantum mechanical systems, but sometimes one may create in artificially fabricated systems such conditions, which are hardly observable "in natura". For example, $1D \to 2D$ crossover may be realized in quantum networks[3] and constrictions[4]. The Kondo effect may be observed in non-equilibrium conditions[5], at high magnetic fields[6], and at finite frequencies[7]. Moreover, a quantum dot in the Kondo regime can be integrated into a circuit exhibiting the Aharonov-Bohm effect[8].

In this paper we focus on an intriguing challenge in this context related to the specific symmetry of the nano-objects under study. More precisely, one is interested in answering questions pertaining to the nature of the underlying symmetry of the dot Hamiltonian and the algebra of operators appearing in the exchange Hamiltonian. The investigation of this topic is intimately related with the geometric structure and electron occupation of the quantum dot in its ground state. We refer to a quantum dot composed of a single well and containing an odd number N of electrons as a *simple* quantum dot (SQD). The dot Hamiltonian of a SQD (in the absence of an external magnetic field) is composed of two degenerate levels and has an $SU(2)$ symmetry. In that sense the symmetry is referred to as geometrical. The exchange Hamiltonian is expressed in terms of the generators of the group $SU(2)$. On the other hand, quantum dots containing a single well with even N or quantum dots containing several wells are referred to as *composite* quantum dots (CQD). The low energy states of an isolated CQD Hamiltonian are spin multiplets. In the generic case, the only degeneracy is that of magnetic quantum numbers. Yet, as we argue below, dot-lead tunneling results in level renormalization and the emergence of an additional degeneracy, both generic and accidental. To be more precise, we note that 1) The exchange part of the Hamiltonian includes the generators of a non-compact Lie group (usually $SO(n)$ or $SU(n)$) and 2) The *renormalized* low-energy spin-excitation levels of the CQD Hamiltonian are almost degenerate (within a Kondo energy scale). These two aspects are gathered under the term *dynamical symmetry*. A more quantitative exposition will be presented below.

Experimentally, resonance Kondo tunneling was observed in QD with odd electron occupation number under strong Coulomb blockade[9], and in individual atoms and molecules deposited on metallic surfaces and on the edges of metallic wires in break-junction geometry[10]. According to the theory of Kondo effect in QD[11], spin degrees of QD are involved in Kondo resonance. In our notation these are SQD and the physics of Kondo tunneling in this case is similar to that of Kondo scattering in magnetically doped metals, at least in the regime of linear

response.

The Kondo physics seems to be richer in systems involving tunneling through CQD. Our main purpose is to demonstrate that CQD possesses dynamical symmetries whose realization in Kondo tunneling is experimentally tangible. Such experimental tuning of dynamical symmetries is not possible in conventional Kondo scattering. In many cases even the very existence of Kondo tunneling crucially depends on the dynamical spin symmetry of CQD. Several models dealing with Kondo tunneling in CQDs possessing dynamical symmetry were considered in our previous publications. The case of $SO(4)$ symmetry in double quantum dot (DQD) was studied in Refs. 12,13. A more complicated case of $SO(n)$ symmetry with variable n in a triple quantum dot (TQD) (composed of three potential valleys with intra-well interaction and inter-well tunneling) is introduced in Ref. 14.

The main goal here is to develop the general approach to the problem of dynamical symmetries in Kondo tunneling through CQDs and illustrate it by numerous examples of TQD in various configurations, both in parallel and in series geometries. Within this framework, our earlier results[14] fit into an elegant pattern of classification of dynamical symmetry groups, which is expanded here in a somewhat more complete and rigorous formalism. The main lesson to be learned is that Kondo physics in CQD suggests a novel and in some sense rather appealing aspect of low-dimensional physics of interacting electrons. It substantiates, in a systematic way, that dynamical symmetry groups play an important role in mesoscopic physics. In particular, we encounter here some "famous" groups which appear in other branches of physics. Thus, the celebrated group $SU(3)$ enters also here when a TQD is subject to an external magnetic field. And the group $SO(5)$ which plays a role in the theory of superconductivity is found here when a certain tuning of the gate voltages in TQD is exercised.

The basic concepts are introduced in section II. First, in sub-section II A, the necessary mathematical ingredients are introduced, although we try to avoid much rigor. Then, in sub-section II B we explain how these abstract concepts can be realized in CQD. In section III the special case of TQD in the *parallel* geometry is discussed at some length. In subsection III A we derive scaling equations for TQD with even occupation and calculate Kondo temperatures for various dynamical symmetries. In section IV we discuss the physics of TQD in a *series* geometry and point out similarities and differences between Kondo physics in the two geometries (sub-section IV A). In sub-section IV B we concentrate on the case of even occupation. The dynamical-symmetry phase diagram is displayed and the experimental consequences are drawn. The case of odd occupation is exposed in subsection IV C. Finally, in section V a novel phenomena is discussed, namely, *a Kondo effect without a localized spin*. The anisotropic exchange interaction occurs between the metal electron spin and the dot Runge-Lenz operator alone. In the conclusions we underscore the main results obtained here.

The derivation of the pertinent effective spin Hamiltonians and the establishment of group properties (in particular identification of the group generators and checking the corresponding commutation relations) sometimes require lengthy mathematical expressions. These are collected in the appendices.

II. DYNAMICAL SYMMETRY OF COMPLEX QUANTUM DOTS

A. Generalities

In this section we present in some details the concept of dynamical symmetry, and more particularly, its emergence in CQD. The term *Dynamical Symmetry* implies the symmetry of eigenvectors of a quantum system forming an irreducible representations of a certain Lie group. The main ideas and the relevant mathematical tools can be found, e.g., in Refs. 15. Here they are formulated in a form convenient for our specific purposes without much mathematical rigor. We have in mind a quantum system with Hamiltonian H whose eigenstates $|\Lambda\rangle = |M\mu\rangle$ form (for a given M) a basis to an irreducible representation of some Lie group $\mathcal{G}$. The energies E_M do not depend on the "magnetic" quantum number μ. For definiteness one may think of M as an angular momentum and of μ as its projection, so that $\mathcal{G}$ is just $SU(2)$. Now let us look for operators which induce transitions between different eigenstates. An economic way for identifying them is through the Hubbard operators[16]

$$X^{\Lambda\Lambda'} = |\Lambda\rangle\langle\Lambda'|. \tag{1}$$

It is natural to divide this set of operators into two subsets . The first one contains the operators $|M\mu\rangle\langle\mu' M|$ while the second one includes operators $|M\mu\rangle\langle\mu' M'|$ for which $|M\mu\rangle$ and $|M'\mu'\rangle$ belong to a *different* representation space of $\mathcal{G}$. A central question at this stage is whether these operators (or rather, certain linear combinations of them) form a close algebra. In some particular cases it is possible to form linear combinations within each set and obtain two new sets of operators $\{S\}$ and $\{R\}$ with the following properties: 1) For a given M the operators $\{S\}$ generate the M irreducible representation of $\mathcal{G}$ and commute with H. 2) For a given set M_i the operators $\{S\}$ and $\{R\}$ form an algebra (the *dynamic* algebra) and generate a non-compact Lie group $\mathcal{A}$. The reason for the adjective *dynamic* is that, originally, the operators $\{R\}$ do not appear in the bare Hamiltonian H and emerge only when additional interaction (e.g., dot-lead tunneling) is present. In the special case $\mathcal{G} = SU(2)$ the operators in $\{S\}$ are the vector $\mathbf{S}$ of spin operators determining the corresponding irreducible representations, while the operators in the set $\{R\}$ can be grouped into a sequence $\mathbf{R}_n$ of vector operators describing transitions

between states belonging to different representations of the $SU(2)$ group.

Strictly speaking, the group $\mathcal{A}$ is not a symmetry group of the Hamiltonian H since the operators $\{R\}$ do not commute with H. Indeed, let us express H in terms of diagonal Hubbard operators,

$$H = \sum_{\Lambda=M\mu} E_\Lambda |\Lambda\rangle\langle\Lambda| = \sum_\Lambda E_M X^{\Lambda\Lambda} \ , \qquad (2)$$

so that

$$[X^{\Lambda\Lambda'}, H] = -(E_M - E_{M'})X^{\Lambda\Lambda'}. \qquad (3)$$

As we have mentioned above, the symmetry group $\mathcal{G}$ of the Hamiltonian H, is generated by the operators $X^{\Lambda=M\mu,\Lambda'=M\mu'}$. Remarkably, however, the dynamics of CQD in contact with metallic leads and/or an external magnetic field leads to renormalization of the energies $\{E_M\}$ in such a way that a few levels at the bottom of the spectrum become degenerate, $E_{M_1} = E_{M_2} = \ldots E_{M_n}$. Hence, in this low energy subspace, the group $\mathcal{A}$ generated by the operators $\{S\}$ and $\{R\}$ is a symmetry group of H referred to as the dynamical symmetry group. The symbol R is due to the analogy with the Runge-Lenz operator, the hallmark of dynamical symmetry of the Kepler and Coulomb problems[17]. Below we will use the term dynamical symmetry also in cases where the levels are not strictly degenerate, their difference is bounded by a certain energy scale, which is the Kondo energy in our special case. In that sense, the symmetry is of course not exact, but rather approximate.

Using the notions of dynamical symmetry, numerous familiar quantum objects, such as hydrogen atom, quantum oscillator in d-dimensions, quantum rotator, may be described in a compact and elegant way. We are interested in a special application of this theory, when the symmetry of the quantum system is approximate and its violation may be treated as a perturbation. This aspect of dynamical symmetry was first introduced in particle physics[18], where the classification of hadron eigenstates is given in terms of non-compact Lie groups. In our case, the rotationally invariant object is an isolated quantum dot, whose spin symmetry is violated by electron tunneling to and from the leads under the condition of strong Coulomb blockade.

B. Realization in CQD

The special cases $\mathcal{G} = SU(2)$ and $\mathcal{A} = SO(n)$ or $SU(n)$ is realizable in CQD. Let us first recall the manner in which the spin vectors appear in the effective low energy Hamiltonian of the QD in tunneling contact with metallic leads. When strong Coulomb blockade completely suppresses charge fluctuations in QD, only spin degrees of freedom are involved in tunneling via the Kondo mechanism[11]. An *isolated* SQD in this regime is represented solely by its spin vector $\mathbf{S}$. This is a manifestation of rotational symmetry which is of geometrical origin. The exchange interaction $J\mathbf{s}\cdot\mathbf{S}$ ($\mathbf{s}$ is the spin operator of the metallic electrons) induces transitions between states belonging to the same spin (and breaks $SU(2)$ invariance). On the other hand, the low energy spectrum of spin excitations in CQD is not characterized solely by its spin operator since there are states close in energy, which belong to different representation spaces of $SU(2)$. Incidentally, these might have either the same spin $\mathbf{S}$ (like, *e.g*, in two different doublets) or a different spin (like, *e.g.*, in the case of singlet-triplet transitions). The exchange interaction must then contain also other operators $\mathbf{R}_n$ (the R-operators mentioned in the previous sections) inducing transitions between states belonging to different representations. The interesting physics occurs when the operators $\mathbf{R}_n$ "approximately" commute with the Hamiltonian H_{dot} of the isolated dot. In accordance with our previous discussion, the R-operators are expressible in terms of Hubbard operators and have only non-diagonal matrix elements in the basis of the eigenstates of H_{dot}. The spin algebra is then a subalgebra of a more general non-compact Lie algebra formed by the whole set of vector operators $\{\mathbf{S}, \mathbf{R}_n\}$. This algebra is characterized by the commutation relations,

$$\begin{aligned} &[S_i, S_j] = it_{ijk}S_k, \quad [S_i, R_{nj}] = it_{ijk}R_{nk}, \\ &[R_{ni}, R_{nj}] = it^n_{ijk}S_k, \end{aligned} \qquad (4)$$

with structure constants t_{ijk}, t^n_{ijk} (here ijk are Cartesian indices). The R-operators are orthogonal to $\mathbf{S}$,

$$\mathbf{S}\cdot\mathbf{R}_n = 0. \qquad (5)$$

In the general case, CQDs possess also other symmetry elements (permutations, reflections, finite rotations). Then, additional scalar generators A_p arise. These generators also may be expressed via the bare Hubbard operators, and their commutation relations with R-operators have the form

$$[R_{ni}, R_{mj}] = ig^{nmp}_{ij}A_p, \quad [R_{ni}, A_p] = if^{nmp}_{ij}R_{mj}, \qquad (6)$$

with structure constants g^{nmp}_{ij} and f^{nmp}_{ij} ($n \neq m$). The operators obeying the commutation relations (4) and (6) form an o_n algebra. The Casimir operator for this algebra is

$$\mathcal{K} = \mathbf{S}^2 + \sum_n \mathbf{R}^2_n + \sum_p A^2_p \ . \qquad (7)$$

Various representations of all these operators via basic Hubbard operators will be established in the following sections, where the properties of specific CQDs are studied.

Next, we show how the dynamical symmetry of CQD is revealed in the effective spin Hamiltonian describing Kondo tunneling. This Hamiltonian is derived from the generalized Anderson Hamiltonian

$$H_A = H_{dot} + H_{lead} + H_{tun}. \qquad (8)$$

The three terms on the right hand side are the dot, lead and tunneling Hamiltonians, respectively. In the generic case, a planar CQD is a confined region of a semiconductor, with complicated multivalley structure secluded between drain and source leads. The CQD contains several valleys numbered by index a. Some of these valleys are connected with each other by tunnel channels characterized by coupling constants $W_{aa'}$, and some of them are connected with the leads by tunneling. The corresponding tunneling matrix elements are V_{ab} ($b = s, d$ stands for source and drain, respectively). The total number of electrons N in a *neutral* CQD as well as the partial occupation numbers N_a for the separate wells are regulated by Coulomb blockade and gate voltages v_{ga} applied to these wells, with $N = \sum_a N_a$. It is assumed that the capacitive energy for the whole CQD is strong enough to suppress charged states with $N' = N \pm 1$, which may arise in a process of lead-dot tunneling.

If the inter-well tunnel matrix elements $W_{aa'}$ are larger than the dot-lead ones V_{ab} (or if all tunneling strengths are comparable), it is convenient first to diagonalize H_{dot} and then consider H_{tun} as a perturbation. In this case H_{dot} may be represented as

$$H_{dot} = \sum_{\Lambda\in N} E_\Lambda |\Lambda\rangle\langle\Lambda| + \sum_{\lambda\in N\pm 1} E_\lambda |\lambda\rangle\langle\lambda|. \qquad (9)$$

Here all intradot interactions are taken into account. The kets $|\Lambda\rangle \equiv |N, q\rangle$ represent eigenstates of H_{dot} in the charge sector N and quantum numbers q, whereas the kets $|\lambda\rangle \equiv |N \pm 1, p\rangle$ are eigenstates in the charge sectors $N \pm 1$ with quantum numbers p. All other charge states are suppressed by Coulomb blockade. Usually, q and p refer to spin quantum numbers but sometimes other specifications are required (see below).

The lead Hamiltonian takes a form

$$H_{lead} = \sum_{k,\alpha,\sigma} \varepsilon_{k\alpha} c^\dagger_{\alpha k\sigma} c_{\alpha k\sigma}. \qquad (10)$$

In the general case, the individual dots composing the CQD are spatially separated, so one should envisage the situation when each dot is coupled by its own channel to the lead electron states. So, the electrons in the leads are characterized by the index α, which specifies the lead (source or drain) and the tunneling channel, as well as by the wave vector k and spin projection σ.

The tunnel Hamiltonian involves electron transfer between the leads and the CQD, and thus couples states $|\Lambda\rangle$ of the dot with occupation N and states $|\lambda\rangle$ of the dot with occupation $N \pm 1$. This is best encoded in terms of non-diagonal dot Hubbard operators, which intermix the states from different *charge sectors*

$$X^{\Lambda\lambda} = |\Lambda\rangle\langle\lambda|, \quad X^{\lambda\Lambda} = |\lambda\rangle\langle\Lambda|. \qquad (11)$$

Thus,

$$H_t = \sum_{k\alpha\sigma} \sum_{\lambda\in N+1, \Lambda\in N} \left(V^{\Lambda\lambda}_{\alpha\sigma} c^\dagger_{\alpha k\sigma} |\Lambda\rangle\langle\lambda| + H.c. \right) + \sum_{k\alpha a\sigma} \sum_{\lambda\in N-1, \Lambda\in N} \left(V^{\lambda\Lambda}_{\alpha\sigma} c^\dagger_{\alpha k\sigma} |\lambda\rangle\langle\Lambda| + H.c. \right), \qquad (12)$$

where $V^{\lambda\Lambda}_{\alpha\sigma} = V_\alpha \langle\lambda| d_{a\sigma} |\Lambda\rangle$.

Before turning to calculation of CQD conductance, the relevant energy scales should be specified. First, we suppose that the bandwidth of the continuum states in the leads, D_α, substantially exceeds the tunnel coupling constants, $D_\alpha \gg W_{aa'}, V_\alpha$ (actually, we consider leads made of the same material with $D_{as} = D_{ad} = D_0$). Second, each well a in the CQD is characterized by the "activation energy" defined as $\Delta_a = E_\Lambda(N_a) - E_\lambda(N_a - 1)$, i.e., the energy necessary to extract one electron from the well containing N_a electrons and move it to the Fermi level of the leads (the Fermi energy is used as the reference zero energy level from now on). Note that Δ_a is tunable by applying the corresponding gate voltage v_{ga}. We are mainly interested in situations where the condition

$$\Delta_c \sim D_0,\ Q_c, \qquad (13)$$

is satisfied at least for one well labeled by the index c. Here Q_c is a capacitive energy, which is predetermined by the radius of the well c. Eventually, this well with the largest charging energy is responsible for Kondo-like effects in tunneling, provided the occupation number N_c is odd. The third condition assumed in our model is a weak enough Coulomb blockade in all other wells except that with $a = c$, i.e., $Q_a \ll Q_c$. Finally, we demand that

$$b_{\alpha a} \equiv \frac{V_\alpha}{\Delta_a} \ll 1, \qquad (14)$$

for those wells, which are coupled with metallic leads, and

$$\beta_a = \frac{W_{ac}}{E_{ac}} \ll 1. \qquad (15)$$

Here E_{ac} are the charge transfer energies for electron tunneling from the c-well to other wells in the CQD.

The interdot coupling under Coulomb blockade in each well generates indirect exchange interactions between electrons occupying different wells. Diagonalizing the dot Hamiltonian for a *given* $N = \sum_a N_a$, one easily finds that the low-lying spin spectrum in the charge sectors with even occupation N consists of singlet/triplet pairs (spin $S = 0$ or 1, respectively). In charge sectors with odd N the manifold of spin states consists of doublets and quartets (spin S=1/2 and 3/2, respectively).

The resonance Kondo tunneling is observed as a temperature dependent zero bias anomaly in tunnel conductance[9]. According to existing theoretical understanding, the quasielastic cotunneling accompanied by the spin flip transitions in a quantum dot is responsible

for this anomaly. To describe the cotunneling through a neutral CQD with given N, one should integrate out transitions involving high-energy states from charge sectors with $N' = N \pm 1$. In the weak coupling regime at $T > T_K$ this procedure is done by means of perturbation theory which can be employed in a compact form within the renormalization group (RG) approach formulated in Refs. 19,20.

As a result of the RG iteration procedure, the energy levels E_Λ in the Hamiltonian (9) are renormalized and indirect exchange interactions between the CQD and the leads arise. The RG procedure is equivalent to summation of the perturbation series at $T > T_K$, where T_K is the Kondo energy characterizing the crossover from a perturbative weak coupling limit to a non-perturbative strong coupling regime. The leading logarithmic approximation of perturbation theory corresponds to a single-loop approximation of RG theory. Within this accuracy the tunnel constants W and V are not renormalized, as well as the charge transfer energy Δ_c (13). Reduction of the energy scale from the initial value D_0 to a lower scale $\sim T$ results in renormalization of the energy levels $E_\Lambda \to \bar{E}_\Lambda(D_0/T)$ and generates an indirect exchange interaction between the dot and the leads with an (antiferromagnetic) exchange constant J.

The rotational symmetry of a *simple* quantum dot is broken by the spin-dependent interaction with the leads, which arises in second order in the tunneling amplitude V_α. In complete analogy, the *dynamical symmetry* of a *composite* quantum dot is exposed (broken) as encoded in the effective exchange Hamiltonian. In a generic case, there are, in fact, several exchange constants arranged within an exchange matrix J which is non-diagonal both in dot and lead quantum numbers. The corresponding exchange Hamiltonian is responsible for spin-flip assisted cotunneling through the CQD as well as for singlet-triplet transitions.

The precise manner in which these statements are quantified will now be explained. After completing the RG procedure, one arrives at an effective (or renormalized) Hamiltonian $\bar{H}$ in a reduced energy scale $\bar{D}$,

$$\bar{H} = \bar{H}_{dot} + \bar{H}_{lead} + \bar{H}_{cotun}, \tag{16}$$

where the effective dot Hamiltonian (9) is reduced to

$$\bar{H}_{dot} = \sum_{\Lambda \in N} \bar{E}_\Lambda X^{\Lambda\Lambda} \tag{17}$$

written in terms of *diagonal* Hubbard operators,

$$X^{\Lambda\Lambda} = |\Lambda\rangle\langle\Lambda|. \tag{18}$$

At this stage, the manifold $\{\Lambda\} \in N$ contains only the renormalized low-energy states within the energy interval comparable with T_K (to be defined below). Some of these states may be quasi degenerate, with energy differences $|\bar{E}_\Lambda - \bar{E}_{\Lambda'}| < T_K$. However, T_K itself is a function of these energy distances (see, e.g.,[6,21,22]), and all the levels, which influence T_K, should be retained in (17).

The effective cotunneling Hamiltonian acquires the form

$$H_{cot} = \sum_{\alpha\alpha'} \left(J_0^{\alpha\alpha'} \mathbf{S} \cdot \mathbf{s}^{\alpha\alpha'} + \sum_n J_n^{\alpha\alpha'} \mathbf{R}_n \cdot \mathbf{s}^{\alpha\alpha'} \right). \tag{19}$$

Here $\mathbf{S}$ is the spin operator of CQD in its ground state, the operators $\mathbf{s}^{\alpha\alpha'}$ represent the spin states of lead electrons,

$$\mathbf{s}^{\alpha\alpha'} = \frac{1}{2} \sum_{kk'} \sum_{\sigma\sigma'} c^\dagger_{\alpha k\sigma} \hat{\tau}_{\sigma\sigma'} c_{\alpha' k'\sigma'} \ , \tag{20}$$

where $\hat{\tau}$ is the vector of Pauli matrices. In the conventional Kondo effect the logarithmic divergent processes develop due to spin reversals given by the first term containing the operator $\mathbf{S}$. In CQD possessing dynamical symmetry, all R-vectors are involved in Kondo tunneling. In the following sections we will show how these additional processes are manifested in resonance Kondo tunneling through CQD. Note that the elements of the matrix J are also subject to temperature dependent renormalization $J_n^{\alpha\alpha'} \to J_n^{\alpha\alpha'}(D_0/T)$.

The cotunneling Hamiltonian (19) is the natural generalization of the conventional Kondo Hamiltonian $J\mathbf{s}\cdot\mathbf{S}$ for CQDs possessing dynamical symmetries. In many cases there are several dot spin 1 operators depending on which pair of electrons is "active". In this pair, one electron sits in well c and the other one sits in some well a. The other $N-2$ electrons are paired in singlet states. This scenario applies if N is even. The spin 1 operator for the active pair is denoted as $\mathbf{S}_a$. (In some sense, the need to specify which pair couples to $S = 1$ while all other pairs are coupled to $S = 0$ is the analog of the seniority scheme in atomic and nuclear physics (see, e.g.,[23])). The cotunneling Hamiltonian for CQD contains exchange terms $J_0^{\alpha\alpha'} \mathbf{S}_a \cdot \mathbf{s}^{\alpha\alpha'}$. Then, instead of a single exchange term (first term on the RHS of Eq. (19)), one has a sum $\sum_a J_a^{\alpha\alpha'} \mathbf{S}_a \cdot \mathbf{s}^{\alpha\alpha'}$. Additional symmetry elements (finite rotations and reflections) turn the cotunneling Hamiltonian even more complicated. In the following sections we will consider several examples of such CQDs. It is seen from (19), that in the generic case, both spin and R-vectors may be the sources of anomalous Kondo resonances. The contribution of these vectors depends on the hierarchy of the energy states in the manifold. In principle, it may happen that the main contribution to the Kondo tunneling is given not by the spin of the dot, but by one of the R-vectors.

Thus, we arrive at the conclusion that the regular procedure of reducing the full Hamiltonian of a quantum dot in junctions with metallic leads to an effective Hamiltonian describing only spin degrees of freedom of this system reveals a rich dynamical symmetry of CQD. Strictly speaking, only an isolated QD with $N = 1$ is fully described by its spin 1/2 operator obeying $SU(2)$ symmetry without dynamical degrees of freedom. Yet even the doubly occupied dot with $N = 2$ possesses the dynamical

symmetry of a *spin rotator* because its spin spectrum consists of a singlet ground state (S) and a triplet excitation (T). Therefore, an R-vector describing S/T transitions may be introduced, and the Kondo tunneling through a dot of this kind may involve spin excitation under definite physical conditions, e.g., in an external magnetic field[6]. A two-electron quantum dot under Coulomb blockade constitutes apparently the simplest non-trivial example of a nano-object with dynamical symmetry of a spin rotator possessing an $SO(4)$ symmetry.

Dynamical symmetries $SO(n)$ of CQDs are described by non-compact semi-simple algebras[24]. This non-compactness implies that the corresponding algebra o_n may be presented as a direct sum of subalgebras, e.g., $o_4 = o_3 \oplus o_3$. Therefore, the dynamical symmetry group may be represented as a direct product of two groups of lower rank. In case of spin rotator the product is $SO(4) = SU(2) \otimes SU(2)$. Generators of these subgroups may be constructed from those of the original group. The $SO(4)$ group possesses a single R-operator $\mathbf{R}$, and the direct product is realized by means of the transformation

$$\mathbf{K} = \frac{\mathbf{S} + \mathbf{R}}{2}, \quad \mathbf{N} = \frac{\mathbf{S} - \mathbf{R}}{2}. \tag{21}$$

Both vectors $\mathbf{K}$ and $\mathbf{N}$ generate $SU(2)$ symmetry and may be treated as fictitious S=1/2 spins[21]. In some situations these vectors are real spins localized in different valleys of CQD. In particular, the transformation (21) maps a single site Kondo problem for a DQD possessing $SO(4)$ symmetry to a two-site Kondo problem for spin 1/2 centers with an $SU(2)$ symmetry (see discussion in Refs. 12,13). For groups of higher dimensionality ($n \geq 4$) one can use many different ways of factorization, which may be represented by means of different Young tableaux (see Appendix D).

Even in the case $n = 4$, the transformation (21) is not the only possible "two-spin" representation. An alternative representation is realized in an external magnetic field[13]. When the ground state of S/T manifold is a singlet (the energy $\delta = E_T - E_S > 0$), the Zeeman splitting energy of a triplet in an external magnetic field may exactly compensate the exchange splitting δ. This occasional degeneracy is described by the pseudospin 1/2 formed by the singlet and the up projection of spin 1 triplet. Two other projections of the triplet form the second pseudospin 1/2. The Kondo effect induced by external magnetic field observed in several nano-objects[25], was the first experimental manifestation of dynamical symmetry in quantum dots.

We outlined in this section the novel features which appear in effective Kondo Hamiltonians due to the dynamical symmetry of CQD exhibiting Kondo tunneling. In the following sections we will see how the additional terms in the Hamiltonian (19) influence the properties of Kondo resonance in various structures of CQDs.

III. TRIPLE QUANTUM DOT IN PARALLEL GEOMETRY

So far we have briefly mentioned a simple structure of CQD, i.e., double quantum dot with occupation $N = 2$ and employed it to describe some generic properties of CQD enumerated in the previous section. This kind of an artificial molecule is the analog of a hydrogen molecule in the Heitler-London limit[12,13], and its $SO(4)$ symmetry reflects the spin properties of ortho/parahydrogen. A much richer artificial object is a triple quantum dot (TQD), which can be considered as an analog of a *linear molecule* RH_2. The central (c) dot is assumed to have a smaller radius (and, hence, larger capacitive energy Q_c) than the left (l) and right (r) dots, i.e., $Q_c \gg Q_{l,r}$. Fig. 1 illustrates this configuration in a parallel geometry, where the "left-right" ($l-r$) reflection plane of the TQD is perpendicular to the "source-drain" ($s-d$) reflection plane of metallic electrodes.

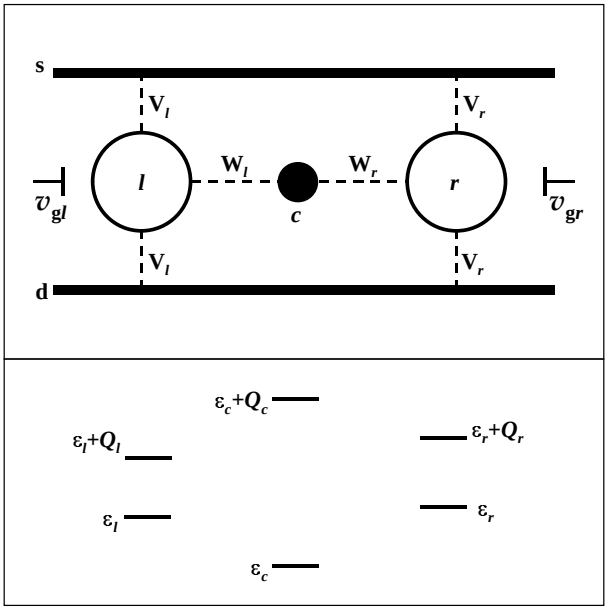

FIG. 1: Triple quantum dot in parallel geometry and energy levels of each dot $\varepsilon_a = \epsilon_a - v_{ga}$ (bare energy minus gate voltage).

To regulate the occupation of TQD as a whole and its constituents in particular, there is a couple of gates v_{gl}, v_{gr} applied to the l, r dots. The energy levels of single- and two-electron states in each one of the three constituent dots are shown in the lower panel of Fig. 1. Here the gate voltages $v_{gl,r}$ are applied in such a way that the one-electron level ϵ_c of a c-dot is essentially deeper than those of the l, r-dots, so that the condition (13) is satisfied for the c dot, whereas the inequalities (14) and (15) are satisfied for the "active" l and r dots. Tunneling between the side dots l, r and the central one c with amplitudes $W_{l,r}$ determines the low energy spin spectrum of the isolated TQD once its occupation N is given. This

system enables the exposure of much richer possibilities for additional degeneracy relative to the DQD setup mentioned above due to the presence of two channels (l, r).

The full diagonalization procedure of the Hamiltonian H_{dot} for the TQD is presented in Appendix A. When the condition (15) is valid, the low-energy manifold for $N = 4$ is composed of two singlets $|S_l\rangle, |S_r\rangle$, two triplets $|T_a\rangle = |\mu_a\rangle$ $(a = l, r, \mu_a = 1_a, 0_a, \bar{1}_a)$ and a charge transfer singlet exciton $|Ex\rangle$ with an electron removed from the c-well to the "outer" wells. Within the first order in $\beta_a \ll 1$ the corresponding energies are,

$$\begin{aligned} E_{S_a} &= \epsilon_c + \epsilon_a + 2\epsilon_{\bar{a}} + Q_{\bar{a}} - 2W_a\beta_a, \\ E_{T_a} &= \epsilon_c + \epsilon_a + 2\epsilon_{\bar{a}} + Q_{\bar{a}}, \\ E_{Ex} &= 2\epsilon_l + 2\epsilon_r + Q_l + Q_r + 2W_l\beta_l + 2W_r\beta_r, \end{aligned} \tag{22}$$

where the charge transfer energies in Eq.(15) (for determining β_a) are $E_{ac} = Q_a + \epsilon_a - \epsilon_c$; the notation $a = l, r$ and $\bar{a} = r, l$ is used ubiquitously hereafter.

The completely symmetric configuration, $\varepsilon_l = \varepsilon_r \equiv \varepsilon$, $Q_l = Q_r \equiv Q$, $W_l = W_r \equiv W$, should be considered separately. In this case the singlet states form even and odd combinations in close analogy with the molecular states $\Sigma^{\pm}$ in axisymmetric molecules. The odd state S_- and two triplet states are degenerate:

$$\begin{aligned} E_{S^+} &= \varepsilon_c + 3\varepsilon + Q - 4W\beta, \\ E_{S^-} &= E_{T_a} = \varepsilon_c + 3\varepsilon + Q, \\ E_{Ex} &= 4\epsilon + 2Q + 4W\beta. \end{aligned} \tag{23}$$

Consideration of these two examples provide us with an opportunity to investigate the dynamical symmetry of CQD.

A. Derivation and solution of scaling equations

We commence with the case of TQD with even occupation $N = 4$ briefly discussed in Ref. 14. This configuration is a direct generalization of an asymmetric spin rotator, i.e., the double quantum dot in a side-bound geometry[12]. Compared with the asymmetric DQD, this composite dot possesses one more symmetry element, i.e., the $l - r$ permutation, which, as will be seen below, enriches the dynamical properties of CQD.

Following a glance at the energy level scheme (22), one is tempted to conclude outright that for finite W, the ground state of this TQD configuration is a singlet and consequently there is no room for the Kondo effect to take place. A more attentive study of the tunneling problem, however, shows that tunneling between the TQD and the leads opens the way for a rich Kondo physics accompanied by numerous dynamical symmetries.

Indeed, inspecting the expressions for the energy levels, one notices that the singlet states E_{S_a} are modified due to inter-well tunneling, whereas the triplet states E_{T_a} are left intact. This difference is due to the admixture of the singlet states with the charge transfer singlet exciton (see Appendix A). As was mentioned in the previous section, the Kondo cotunneling in the perturbative weak coupling regime at $T, \varepsilon > T_K$ is excellently described within RG formalism[19,20]. According to general prescriptions of this theory, the renormalizable parameters of the effective low-energy Hamiltonian in a one-loop approximation are the energy levels E_Λ and the effective indirect exchange vertices $J^{\alpha\alpha'}_{\Lambda\Lambda'}$.

To apply the RG procedure to the Kondo tunneling through TQD, let us first specify the terms H_{lead} and H_{tun} in the Anderson Hamiltonian (8). The most interesting for us are situations where the accidental degeneracy of spin states is realized. So we consider geometries where the device *as a whole* possesses either complete or slightly violated $l - r$ axial symmetry. Then the quantum number α in H_{lead} (10) contains the lead index (s, d) and the channel index (l, r). If the axial $l - r$ symmetry is perfect, the two tunneling channels are independent. To describe weak violation of this symmetry we introduce weak interchannel hybridization in the leads. This hybridization is characterized by a constant $t_{lr} \ll D_0$, which is small first due to the angular symmetry, and second due to significant spatial separation between the two channels. The wave vector k is assumed to remain a good quantum number. Then, having in mind that in our model $\epsilon_{kas} = \epsilon_{kad} \equiv \epsilon_{ka}$, the generalized Hamiltonian (10) acquires the form

$$H_{lead} = \sum_{k\sigma} \sum_{b=s,d} \sum_{a=l,r} \left(\epsilon_{ka} n_{abk\sigma} + t_{lr} c^\dagger_{abk\sigma} c_{\bar{a}bk\sigma} \right). \tag{24}$$

The tunneling Hamiltonian (12) is written as

$$H_{tun} = \sum_{\Lambda\lambda} \sum_{k\sigma} \sum_{ab} (V^{\lambda\Lambda}_{ab\sigma} c^\dagger_{abk\sigma} X^{\lambda\Lambda} + H.c.). \tag{25}$$

We assume below $V_{as} = V_{ad} \equiv V_a$ (see Fig.1).

The iteration processes, which characterize the two-step RG procedure contributing to these parameters are illustrated in Fig.2. The intermediate states in these diagrams are the high-energy states $|q\rangle$ near the ultraviolet cut-off energy D of the band continuum in the leads (dashed lines) and the states $|\lambda\rangle \in N - 1$ from adjacent charge sectors, which are admixed with the low-energy states $|\Lambda\rangle \in N$ by the tunneling Hamiltonian H_t (12) (full lines). For the sake of simplicity we confine ourselves with $N = 3$ states in the charge sector.

In the upper panel, the diagrams contributing to the renormalization of H_{dot} are shown. In comparison with the original theory[20], this procedure not only results in renormalization of the energy levels but also an additional hybridization of the states $|\Lambda_a\rangle$ via channel mixing terms in the Hamiltonian (25). Due to the condition (13), the central dot c remains "passive" throughout the RG procedure.

The mathematical realization of the diagrams displayed in Fig.2a is encoded in the scaling equations for

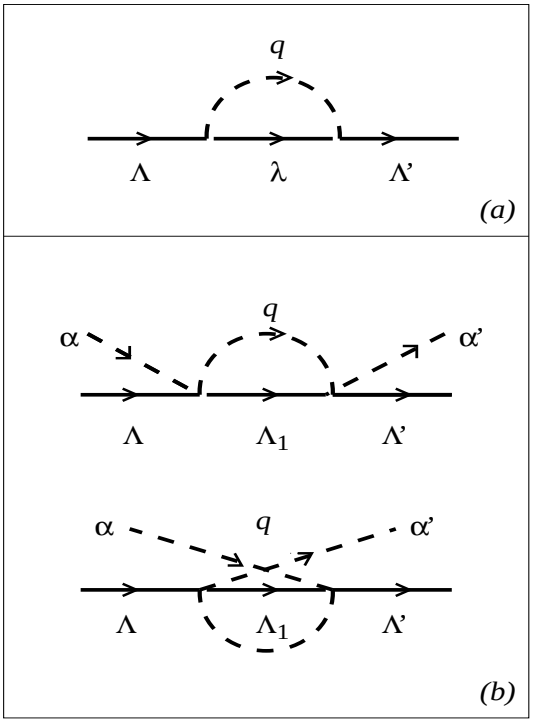

FIG. 2: RG diagrams for the energy levels E_Λ (a) and the effective exchange vertices $J^{\alpha\alpha'}_{\Lambda\Lambda'}$ (b) (see text for further explanations).

the energy levels E_Λ,

$$\pi\, dE_\Lambda/dD = \sum_\lambda \frac{\Gamma_\Lambda}{D - E_{\Lambda\lambda}}. \tag{26}$$

Here $E_{\Lambda\lambda} = E_\Lambda - E_\lambda$, Γ_Λ are the tunnel coupling constants which are different for different Λ,

$$\Gamma_{T_a} = \pi\rho_0(V_a^2 + 2V_{\bar a}^2), \qquad \Gamma_{S_a} = \alpha_a^2\Gamma_{T_a}. \tag{27}$$

Here $\alpha_a = \sqrt{1-2\beta_a^2}$, and ρ_0 is the density of electron states in the leads, which is supposed to be energy independent. These scaling equations should be solved at some initial conditions

$$E_\Lambda(D_0) = E_\Lambda^{(0)}, \tag{28}$$

where the index (0) marks the bare values of the model parameters entering the Hamiltonian H_A (8).

Besides, the diagram of Fig.2a generates a new vertex $M_{lr}^{\Lambda\Lambda'}$, where the states Λ, Λ' are either two singlets S_l, S_r or two triplets T_l, T_r. The Haldane's iteration procedure results in a scaling equation

$$dM_{lr}/d\ln D = -\gamma \tag{29}$$

with the initial condition $M_{lr}(D_0) = 0$ and the flow rate $\gamma = \rho_0^2 V_l V_r t_{lr}$. After performing the Haldane's procedure we formally come to the scaled dot Hamiltonian

$$H = \sum_{\Lambda_a} E_{\Lambda_a} X^{\Lambda_a\Lambda_a} + \sum_{\Lambda_a\Lambda_{\bar a}} M_{lr} X^{\Lambda_a\Lambda_{\bar a}} \tag{30}$$

with the parameters E_{Λ_a} and M_{lr} depending on the running variable D.

Due to the above mentioned dependence of tunneling rates on the index Λ, namely the possibility of $\Gamma_T > \Gamma_S$ and $\Gamma_{S_-} > \Gamma_{S_+}$, the scaling trajectories $E_\Lambda(D)$ may cross at some value of the monotonically decreasing energy parameter D. The nature of level crossing is predetermined by the initial conditions (28) and the ratios between the tunneling rates Γ_Λ. As long as the inequality $|E_{\Lambda\lambda}| \ll D$ is effective and all levels are non-degenerate, the scaling equations (26) may be approximated as

$$\pi\, dE_\Lambda/d\ln D = \Gamma_\Lambda. \tag{31}$$

The scaling trajectories are determined by the scaling invariants for equations (26),

$$E_\Lambda^* = E_\Lambda(D) - \pi^{-1}\Gamma_\Lambda \ln(\pi D/\Gamma_\Lambda), \tag{32}$$

tuned to satisfy the initial conditions. With decreasing energy scale D these trajectories flatten and become D-independent in the so called Schrieffer-Wolff (SW) limit, which is reached when the activation energies Δ_a become comparable with D. The corresponding effective bandwidth is denoted as $\bar D$ (we suppose, for the sake of simplicity, that $\Delta_a < Q_a$, so that only the states $|\lambda\rangle$ with $N' = N-1$ are relevant). The simultaneous evolution of interchannel hybridization parameter is described by the solution of scaling equation (29),

$$M_{lr}(\bar D) = \gamma \ln \frac{D_0}{\bar D}. \tag{33}$$

If this remarkable level crossing occurs at $D > \bar D$, we arrive at the situation where *adding an indirect exchange interaction between the TQD and the leads changes the magnetic state of the TQD from singlet to triplet*. Those states E_Λ, which remain close enough to the new ground state are involved in the Kondo tunneling. As a result, the TQD acquires a rich dynamical symmetry structure instead of the trivial symmetry of spin singlet predetermined by the initial energy level scheme (22). Appearance of the logarithmic enhancement of the hybridization parameter M_{lr} (33) does not radically influence the general picture, provided the flow trajectories cross far from the SW line , due to a very small hybridization $\gamma \ll \Gamma_\Lambda \ll D$. However, we are interested just in cases when the accidental degeneracy occurs at the SW line. Various possibilities of this degeneracy are considered below.

The flow diagrams leading to a non-trivial dynamical symmetry of TQD with $N = 4$ are presented in Figs.3,5,6. The horizontal axis on these diagrams is the current energy scale D for lead electrons, where the vertical axes represent the energy levels $E_\Lambda(D)$. The dashed line $E = -D$ establishes the SW boundary for these levels.

Before turning to highly degenerate situations, where the system possesses specific $SO(n)$ symmetry, it is instructive to consider the general case, where all flow trajectories $E_\Lambda(\bar D)$ are involved in Kondo tunneling in the

SW limit. This happens when the whole octet of spin singlets and triplets forming the manifold (22) remains within the energy interval $\sim T_K$ in the SW limit. The level repulsion effect does not prevent formation of such multiplet, provided t_{lr} is small enough and the inequality

$$M_{lr}(\bar{D}) < T_K \tag{34}$$

is valid. At this stage, the SW procedure for constructing the effective spin Hamiltonian in the subspace $\mathbb{R}_8 = \{T_l, S_l, T_r, S_r\}$ should be applied. This procedure excludes the charged states generated by H_t to second order in perturbation theory (see, e.g.,[26]).

The effective cotunneling Hamiltonian can be derived using Schrieffer-Wolf procedure[27] (see Appendix C). To simplify the SW transformation, one should first rationalize the tunneling matrix V in the Hamiltonian (25). This 4×4 matrix is diagonalized in the $s-d, l-r$ space by means of the transformation to even/odd combinations of lead electron k-states and similar symmetric/antisymmetric combinations of l, r electrons in the dots. The form of this transformation for symmetric TQD can be found in Appendix B. Like in the case of conventional QD[11], this transformation eliminates the odd combination of $s-d$ electron wave functions from tunneling Hamiltonian.

It should be emphasized that this transformation does not exclude the odd component from H_{tun} in case of TQD in a series geometry[28]. The same is valid for the Hamiltonians (24), (25) with $t_{lr} = 0$: in this case the rotation in $s-d$ space conformally maps the Hamiltonian H_A (8) for TQD in parallel geometry onto that for TQD in series. Both these cases will be considered in Section IV.

Unlike the case of DQD studied in Refs. 12,13, where the spin operators are the total spin $\mathbf{S}$ and a single R-operator, describing S/T transitions, the TQD is represented by several spin operators corresponding to different Young tableaux (see Appendix D). To order $O(|V|^2)$, then,

$$\begin{aligned} H_{cot} &= \sum_{\Lambda_a} \bar{E}_{\Lambda_a} X^{\Lambda_a\Lambda_a} + \sum_{\Lambda_a\Lambda_{\bar{a}}} \bar{M}_{lr} X^{\Lambda_a\Lambda_{\bar{a}}} \\ &+ \sum_{k\sigma} \sum_{b=s,d} \sum_{a=l,r} \left(\epsilon_{ka} n_{abk\sigma} + t_{lr} c^+_{abk\sigma} c_{\bar{a}bk\sigma}\right) \\ &+ \sum_{a=l,r} J^T_a \mathbf{S}_a \cdot \mathbf{s}_a + J_{lr} \hat{P} \sum_{a=l,r} \mathbf{S}_a \cdot \mathbf{s}_{\bar{a}a} \\ &+ \sum_{a=l,r} J^{ST}_a \mathbf{R}_a \cdot \mathbf{s}_a + J_{lr} \sum_{a=l,r} \tilde{\mathbf{R}}_a \cdot \mathbf{s}_{a\bar{a}}. \end{aligned} \tag{35}$$

Here we recall that $\bar{E}_{\Lambda_a} = E_{\Lambda_a}(\bar{D})$, $\bar{M}_{lr} = M_{lr}(\bar{D})$, and the effective exchange constants are

$$\begin{aligned} J^T_a &= \frac{V_a^2}{\epsilon_F - \epsilon_a}, \qquad J^{ST}_a = \alpha_a J^T_a, \\ J_{lr} &= \frac{V_l V_r}{2} \left(\frac{1}{\epsilon_F - \epsilon_l} + \frac{1}{\epsilon_F - \epsilon_r}\right). \end{aligned} \tag{36}$$

The vector operators $\mathbf{S}_a, \mathbf{R}_a, \tilde{\mathbf{R}}_a$ and the permutation operator $\hat{P}$ manifest the dynamical symmetry of TQD in a subspace $\mathbb{R}_8$. The permutation operator

$$\hat{P} = \sum_{a=l,r} \left(X^{S_a S_{\bar{a}}} + \sum_{\mu=1,0,\bar{1}} X^{\mu_a \mu_{\bar{a}}}\right) \tag{37}$$

commutes with $\mathbf{S}_l + \mathbf{S}_r$ and $\mathbf{R}_l + \mathbf{R}_r$.

The spherical components of these vectors are defined via Hubbard operators connecting different states of the octet,

$$\begin{aligned} S^+_a &= \sqrt{2}(X^{1_a 0_a} + X^{0_a \bar{1}_a}), & S^-_a &= (S^+_a)^\dagger, \\ S^z_a &= X^{1_a 1_a} - X^{\bar{1}_a \bar{1}_a} \\ R^+_a &= \sqrt{2}(X^{1_a S_a} - X^{S_a \bar{1}_a}), & R^-_a &= (R^+_a)^\dagger, \\ R^z_a &= -(X^{0_a S_a} + X^{S_a 0_a}), \\ \tilde{R}^+_a &= \sqrt{2}(\alpha_{\bar{a}} X^{1_a S_{\bar{a}}} - \alpha_a X^{S_a \bar{1}_{\bar{a}}}), & \tilde{R}^-_a &= (\tilde{R}^+_a)^\dagger, \\ \tilde{R}^z_a &= -(\alpha_{\bar{a}} X^{0_a S_{\bar{a}}} + \alpha_a X^{S_a 0_{\bar{a}}}). \end{aligned} \tag{38}$$

In addition to the spin operator (20) for conduction electrons, new spin operators are required,

$$\mathbf{s}_{a\bar{a}} = \frac{1}{2} \sum_{kk'} \sum_{\sigma\sigma'} c^\dagger_{ak\sigma} \hat{\tau}_{\sigma\sigma'} c_{\bar{a}k'\sigma'}. \tag{39}$$

An extra symmetry element (l-r permutation) results in more complicated algebra which involves new R-operator $\tilde{\mathbf{R}}$ and the permutation operator $\hat{P}$ interchanging l and r components of TQD.

One can derive from the generic Hamiltonian (35) more symmetric effective Hamiltonians describing partly degenerate configurations illustrated by the flow diagrams of Figs. 3,5,6. These are the cases when the level crossing occurs in a nearest vicinity of the SW line in the flow diagram. It is important to distinguish between the cases of generic and accidental symmetry. In the former case the device possesses intrinsic $l-r$ and $s-d$ symmetry, i.e., the left and right dots are identical, the corresponding tunnel parameters are equal, and left and right leads also mirror each other, namely, $\epsilon_{kl} = \epsilon_{kr} \equiv \epsilon_k$. In the latter case the gate voltages violates $l-r$ symmetry, e.g., make $\epsilon_l \neq \epsilon_r$, $V_l \neq V_r$, etc. The level degeneracy is achieved due to competition between the $l-r$ interdot tunneling and the lead-dot tunneling without changing the symmetry of the Hamiltonian.

The basic spin Hamiltonian (35) acquires a more compact form, when a TQD possesses generic or accidental degeneracy. In these cases the operators (38) form close algebras, which predetermine the dynamical symmetry of Kondo tunneling. We start the discussion of the pertinent $SO(n)$ symmetries with the most degenerate configuration (Fig. 3), where the TQD possesses generic $l-r$ axial symmetry, i.e., the left and right dots are completely equivalent. Then the energy spectrum of an isolated TQD is given by Eqs.(23). The four-electron wave functions are calculated in Appendix (A). Such TQD is a straightforward generalization of the so called

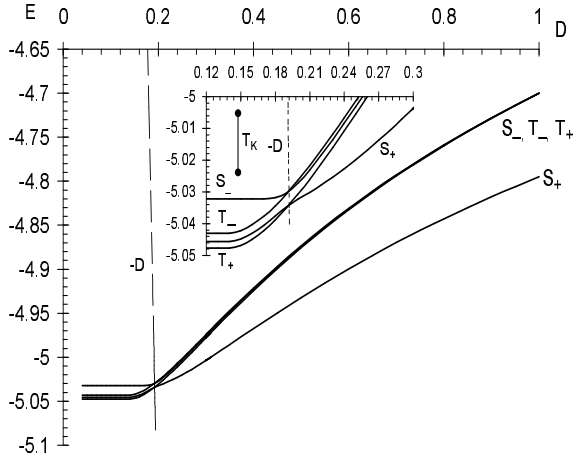

FIG. 3: Scaling trajectories for $P\times SO(4)\times SO(4)$ symmetry in the SW regime. Inset: Zoomed in avoided level crossing pattern near the SW line

T-shaped DQD introduced in Refs. 12,13,29. It is clear, that attachment of a third dot simply adds one more element to the symmetry group $SO(4)$, namely the $l-r$ permutation $\hat{P}$, which is parity sensitive.

To reduce the Hamiltonian (35) into a more symmetric form, we rewrite the Hubbard operators in terms of new eigenstates $\bar{E}_\Lambda$, recalculated with account of generic degeneracy (23) and $l-r$ mixing $\bar{M}_{lr}$. In assuming that the latter coupling parameter is the smallest one, it results in insignificant additional remormalization $\sim \mp|\bar{M}_{lr}|^2/(\varepsilon+Q-\varepsilon_c)$ of the states E_{S+} and E_{Ex}. Besides, it intermixes the triplet states and changes their nomenclature from left/right to even/odd. The corresponding energy levels are

$$E_{T\pm}(\bar{D}) = E_{T_a} \mp \bar{M}_{lr}. \tag{40}$$

The flow trajectories for two pairs of states (T_+,T_-) and (S_+,S_-) diverge slowly with decreasing D. If this divergence is negligible in the scale of T_K, then three nearly coincident trajectories $E_{T\pm},E_{S_-}$ cross the fourth trajectory E_{S+} at some point, since the inequality $\Gamma_{S_+}<\Gamma_{T\pm}=\Gamma_{S-}$ with $\Gamma_{T\pm}=3\pi\rho_o V^2$, $\Gamma_{S_+}=\alpha\Gamma_{T\pm}$ is valid ($\alpha=\sqrt{1-4\beta^2}$). If this level crossing happens near the SW line, we arrive at a case of complete degeneracy of the renormalized spectrum, and the whole octet $\mathbb{R}_8$ is involved in the dynamical symmetry (Fig. 3). The fine structure of the flow diagram in the region of avoided level crossing is shown in the inset.

Since the tunneling occurs in even and odd channels independently, the parity is conserved also in indirect SW exchange. As a result, the effective spin Hamiltonian (35) acquires the form

$$\begin{aligned} H_{cot} &= \sum_{\Lambda_\eta}\bar{E}_{\Lambda_\eta}X^{\Lambda_\eta\Lambda_\eta}+\sum_{k\sigma}\sum_{\eta=g,u}\epsilon_{k\eta}c^\dagger_{\eta k\sigma}c_{\eta k\sigma} \\ &+\sum_{\eta=g,u}J^T_{1\eta}\mathbf{S}_\eta\cdot\mathbf{s}_\eta+\sum_{\eta=g,u}J^{ST}_{1\eta}\mathbf{R}_\eta\cdot\mathbf{s}_\eta \\ &+J^T_2\sum_\eta\mathbf{S}_{\eta\bar{\eta}}\cdot\mathbf{s}_{\eta\bar{\eta}}+\sum_\eta(J^{ST}_{2\eta}\mathbf{R}^{(1)}_{\eta\bar{\eta}}+J^{ST}_{2\bar{\eta}}\mathbf{R}^{(2)}_{\eta\bar{\eta}})\cdot\mathbf{s}_{\eta\bar{\eta}}. \end{aligned} \tag{41}$$

Here $\epsilon_{kg}=\epsilon_k-t_{lr}$, $\epsilon_{ku}=\epsilon_k+t_{lr}$ and the lead operators $c_{\eta k\sigma}$ $(\eta=g,u)$ are defined in Appendix B. The operators $\mathbf{S}_\eta$, $\mathbf{R}_\eta$ are defined analogously to $\mathbf{S}_a$, $\mathbf{R}_a$ in Eq.(38), and the vector operators $\mathbf{S}_{\eta\bar{\eta}}$, $\mathbf{R}^{(1)}_{\eta\bar{\eta}}$, $\mathbf{R}^{(2)}_{\eta\bar{\eta}}$ are defined as:

$$\mathbf{S}_{\eta\bar{\eta}} = X^{\eta\bar{\eta}}\mathbf{S}_{\bar{\eta}}, \qquad \mathbf{R}^{(1)}_{\eta\bar{\eta}}+\mathbf{R}^{(2)}_{\eta\bar{\eta}}=X^{\eta\bar{\eta}}\mathbf{R}_{\bar{\eta}}. \tag{42}$$

The spherical components of the operators $\mathbf{R}^{(1)}_{\eta\bar{\eta}}$ and $\mathbf{R}^{(2)}_{\eta\bar{\eta}}$ are given by

$$\begin{aligned} R^{(1)+}_{\eta\bar{\eta}} &= -\sqrt{2}X^{S_\eta\bar{1}_{\bar{\eta}}}, \qquad R^{(1)-}_{\eta\bar{\eta}}=(R^{(1)+}_{\eta\bar{\eta}})^\dagger, \\ R^{(2)+}_{\eta\bar{\eta}} &= \sqrt{2}X^{1_\eta S_{\bar{\eta}}}, \qquad R^{(2)-}_{\eta\bar{\eta}}=(R^{(2)+}_{\eta\bar{\eta}})^\dagger, \\ R^{(1)z}_{\eta\bar{\eta}} &= -X^{S_\eta 0_{\bar{\eta}}}, \qquad R^{(2)z}_{\eta\bar{\eta}}=-X^{0_\eta S_{\bar{\eta}}}. \end{aligned} \tag{43}$$

The spin operators for the electrons in the leads are introduced by the obvious relations

$$\begin{aligned} \mathbf{s}_g &= \frac{1}{2}\sum_{kk'}\sum_{\sigma\sigma'}c^\dagger_{gk\sigma}\hat{\tau}_{\sigma\sigma'}c_{gk'\sigma'}, \\ \mathbf{s}_u &= \frac{1}{2}\sum_{kk'}\sum_{\sigma\sigma'}c^\dagger_{uk\sigma}\hat{\tau}_{\sigma\sigma'}c_{uk'\sigma'}, \\ \mathbf{s}_{gu} &= \frac{1}{2}\sum_{kk'}\sum_{\sigma\sigma'}c^\dagger_{gk\sigma}\hat{\tau}_{\sigma\sigma'}c_{uk'\sigma'}, \quad \mathbf{s}_{ug}=(\mathbf{s}_{gu})^\dagger, \end{aligned} \tag{44}$$

instead of (20). Now the operator algebra is given by the closed system of commutation relations which is a generalization of the o_4 algebra,

$$\begin{aligned} &[S_{\eta j},S_{\eta' k}]=ie_{jkm}\delta_{\eta\eta'}S_{\eta m}, \\ &[R_{\eta j},R_{\eta' k}]=ie_{jkm}\delta_{\eta\eta'}S_{\eta m}, \\ &[R_{\eta j},S_{\eta' k}]=ie_{jkm}\delta_{\eta\eta'}R_{\eta m}. \end{aligned} \tag{45}$$

The operators $\mathbf{S}_\eta$ are orthogonal to $\mathbf{R}_\eta$, and the Casimir operators in this case are $\mathcal{K}_\eta=\mathbf{S}^2_\eta+\mathbf{R}^2_\eta=3$. This justifies the qualification of such TQD as a *double spin rotator* which is obtained from the spin rotator considered in Refs.[12,13] by a mirror reflection. The symmetry of such TQD is $P\times SO(4)\times SO(4)$.

Four additional vertices appear in the effective spin Hamiltonian (41) at the second stage of Haldane-Anderson scaling procedure[19]. As a result, the exchange part of the Hamiltonian (41) takes the form

$$\begin{aligned} H_{cot} &= \sum_{\eta=g,u}J^T_{1\eta}\mathbf{S}_\eta\cdot\mathbf{s}_\eta+\sum_{\eta=g,u}J^{ST}_{1\eta}\mathbf{R}_\eta\cdot\mathbf{s}_\eta \\ &+J^T_2\sum_\eta\mathbf{S}_{\eta\bar{\eta}}\cdot\mathbf{s}_{\eta\bar{\eta}}+\sum_\eta(J^{ST}_{2\eta}\mathbf{R}^{(1)}_{\eta\bar{\eta}}+J^{ST}_{2\bar{\eta}}\mathbf{R}^{(2)}_{\eta\bar{\eta}})\cdot\mathbf{s}_{\eta\bar{\eta}} \\ &+\sum_\eta J^T_{3\eta}\mathbf{S}_\eta\cdot\mathbf{s}_{\bar{\eta}}+\sum_\eta J^{ST}_{3\eta}\mathbf{R}_\eta\cdot\mathbf{s}_{\bar{\eta}}. \end{aligned} \tag{46}$$

The coupling constants in the Hamiltonian (46) are subject to renormalization. Their values at $D = \bar{D}$ are taken as a boundary conditions

$$J^T_{1\eta}(\bar{D}) = J^T_2(\bar{D}) = J^{ST}_{1u}(\bar{D}) = J^{ST}_{2u}(\bar{D}) = \frac{V^2}{\epsilon_F - \epsilon}, \quad (47)$$
$$J^T_{3\eta}(\bar{D}) = J^{ST}_{3u}(\bar{D}) = 0, \; J^{ST}_{ig}(\bar{D}) = \alpha J^T_{ig}(\bar{D}) \; (i = 1, 2, 3)$$

for solving the scaling equations. These can be written in the following form:

$$\begin{aligned}
\frac{dj^T_{1\eta}}{d\ln d} &= -\Big[(j^T_{1\eta})^2 + 2(-1)^\eta m_{lr} j^T_{1\eta} \\
&+ (j^{ST}_{1\eta})^2 + \frac{(j^T_2)^2}{2} + \frac{(j^{ST}_{2\bar{\eta}})^2}{2}\Big], \\
\frac{dj^T_2}{d\ln d} &= -\frac{1}{2}\Big[\sum_{\eta=g,u}\{j^T_2(j^T_{1\eta} + j^T_{3\eta}) + j^{ST}_{2\eta}(j^{ST}_{1\eta} + j^{ST}_{3\eta})\}\Big], \\
\frac{dj^T_{3\eta}}{d\ln d} &= -\Big[(j^T_{3\eta})^2 + 2(-1)^\eta m_{lr} j^T_{3\eta} \\
&+ (j^{ST}_{3\eta})^2 + \frac{(j^T_2)^2}{2} + \frac{(j^{ST}_{2\bar{\eta}})^2}{2}\Big], \\
\frac{dj^{ST}_{1\eta}}{d\ln d} &= -\Big[2j^T_{1\eta} j^{ST}_{1\eta} + 2(-1)^\eta m_{lr} j^{ST}_{1\eta} + j^T_2 j^{ST}_{2\eta}\Big], \\
\frac{dj^{ST}_{2\eta}}{d\ln d} &= -\frac{1}{2}\Big[\sum_\eta j^T_2(j^{ST}_{1\eta} + j^{ST}_{3\eta}) + 2j^{ST}_{2\eta}(j^T_{1\bar{\eta}} + j^T_{3\bar{\eta}})\Big], \\
\frac{dj^{ST}_{3\eta}}{d\ln d} &= -\Big[2j^T_{3\eta} j^{ST}_{3\eta} + 2(-1)^\eta m_{lr} j^{ST}_{3\eta} + j^T_2 j^{ST}_{2\eta}\Big], \quad (48)
\end{aligned}$$

where $j_{i\eta} = \rho_0 J_{i\eta}$ $(i = 1, 2, 3)$, $d = \rho_0 D$ and $m_{lr} = \rho_0 M_{lr}$.

Solution of Eqs. (48) yields the Kondo temperature

$$T_{K0} = \bar{D}\left(1 - \frac{8m_{lr}}{(\sqrt{3}+1)(3j^T_{1g} + j^{ST}_{1g})}\right)^{\frac{1}{2m_{lr}}}. \quad (49)$$

The limiting value of this relation for perfect $l - r$ symmetry of the leads is

$$\lim_{m_{lr}\to 0} T_{K0} = \bar{D}\exp\left(-\frac{4}{(\sqrt{3}+1)(3j^T_{1g} + j^{ST}_{1g})}\right). \quad (50)$$

Here and below the coupling constants $j_i(D)$ in all equations for T_K are taken at $D = \bar{D}$. We see that avoided crossing effect in the case of slightly violated $l - r$ symmetry of TQD turns the Kondo temperature to be a function of the level splitting (40). Similar situation has been noticed in previous studies of DQD[12,13] and planar QD with even occupation[6], where T_K turned out to be a monotonically decreasing function of S/T splitting energy $\delta = \bar{E}_S - \bar{E}_T$ with a maximum at $\delta = 0$. Now the Kondo temperature is a function of two parameters, $T_K(M_{lr}, \delta)$. Looking at Fig.3 (which corresponds to $\delta = 0$) we notice that for large enough M_{lr}, when the inequality (34) is violated, $M_{lr} \gg T_K$, the symmetry of TQD is reduced to $SO(4)$ symmetry of S/T manifold with the Kondo temperature

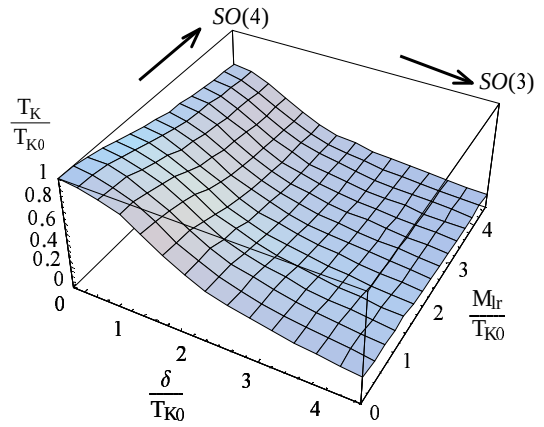

FIG. 4: Variation of T_K with parameters δ and M_{lr} (see text for further details).

$$T_{K1} = \bar{D}\exp\left\{-\frac{1}{j^T_1 + j^{ST}_1}\right\}. \quad (51)$$

Additional S/T splitting induced by the gate voltage ($\epsilon_l \neq \epsilon_r$) results in further decrease of T_K as a function of δ. The asymptotic form of the function $T_K(\delta)$ is

$$\frac{T_K}{T_{K1}} \approx \left(\frac{T_{K1}}{\delta}\right)^\alpha \quad (52)$$

(cf.[6,21]). In the limit of $\delta \to \bar{D}$ the singlet state should be excluded from the manifold, and the symmetry of the TQD with spin one in this case is $SO(3)$. The general shape of $T_K(M_{lr}, \delta)$ surface is presented in Fig.4. Thus the Kondo effect for the TQD with mirror symmetry is characterized by the stable infinite fixed point characteristic for the *underscreened* spin one dot, similar to that for DQD[12,13].

Now we turn to asymmetric configurations where $E_{lc} \neq E_{rc}$, $\Gamma_{T_r} \neq \Gamma_{T_l}$. In this case the system loses the $l - r$ symmetry, and it is more convenient to return to the initial variables used in the generic Hamiltonian (35).

When the Haldane renormalization results in *accidental* degeneracy of two singlets and one triplet, $\bar{E}_{S_l} \approx \bar{E}_{T_l} \approx \bar{E}_{S_r} < \bar{E}_{T_r}$ (Fig. 5), the TQD acquires an $SO(5)$ symmetry of a manifold $\{T_l, S_l, S_r\}$. In this case the SW Hamiltonian (35) transforms into

$$\begin{aligned}
H &= \sum_{\Lambda=T_l,S_l,S_r} \bar{E}_\Lambda X^{\Lambda\Lambda} + M_{lr}(X^{S_l S_r} + X^{S_r S_l}) \quad (53) \\
&+ \sum_{k\sigma}\sum_{a=l,r} \epsilon_{ka} c^+_{ak\sigma} c_{ak\sigma} + t_{lr}\sum_{k\sigma}\sum_{a=l,r} c^+_{ak\sigma} c_{\bar{a}k\sigma} \\
&+ J_1 \mathbf{S}_l \cdot \mathbf{s}_l + J_2 \mathbf{R}_l \cdot \mathbf{s}_l + J_3(\tilde{\mathbf{R}}_1 \cdot \mathbf{s}_{rl} + \tilde{\mathbf{R}}_2 \cdot \mathbf{s}_{lr}),
\end{aligned}$$

where $J_1 = J^T_l$, $J_2 = J^{ST}_l$ and $J_3 = \alpha_r J_{lr}$. The spherical components of the vector operators $\tilde{\mathbf{R}}_1$ and $\tilde{\mathbf{R}}_2$ are given

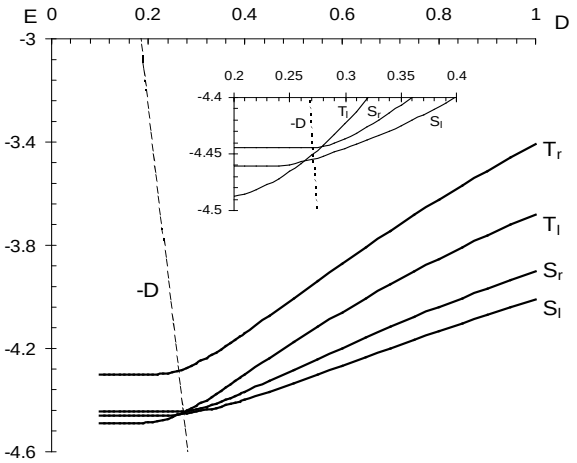

FIG. 5: Scaling trajectories resulting in an $SO(5)$ symmetry in the SW regime. Inset: Zoomed in avoided level crossing pattern near the SW line.

by the following expressions,

$$\tilde{R}_1^+ = -\sqrt{2}X^{S_r\bar{1}_l},\ \tilde{R}_1^- = \sqrt{2}X^{S_r 1_l},\ \tilde{R}_{1z} = -X^{S_r 0_l},$$
$$\tilde{R}_2^+ = (\tilde{R}_1^-)^\dagger, \qquad \tilde{R}_2^- = (\tilde{R}_1^+)^\dagger, \qquad \tilde{R}_{2z} = \tilde{R}_{1z}^\dagger. \quad (54)$$

The group generators of the o_5 algebra are the l-vectors $\mathbf{S}_l, \mathbf{R}_l$ from (38) and the operators intermixing l- and r-states, namely the vector $\tilde{\mathbf{R}} = \tilde{\mathbf{R}}_1 + \tilde{\mathbf{R}}_2$,

$$\tilde{R}^+ = \sqrt{2}(X^{1_l S_r} - X^{S_r\bar{1}_l}),\ \ \tilde{R}^- = (\tilde{R}^+)^\dagger,$$
$$\tilde{R}^z = -(X^{0_l S_r} + X^{S_r 0_l}), \quad (55)$$

and a scalar A interchanging l, r variables of degenerate singlets

$$A = i(X^{S_r S_l} - X^{S_l S_r})\ . \quad (56)$$

The commutation relations (4),(6) in this particular case acquire the form

$$[S_{lj}, S_{lk}] = ie_{jkm}S_{lm}, \qquad [R_{lj}, R_{lk}] = ie_{jkm}S_{lm},$$
$$[\tilde{R}_j, S_{lk}] = ie_{jkm}\tilde{R}_m, \qquad [\tilde{R}_j, \tilde{R}_k] = ie_{jkm}S_{lm},$$
$$[R_{lj}, S_{lk}] = ie_{jkm}R_{lm}, \qquad [R_{lj}, \tilde{R}_k] = i\delta_{jk}A, \quad (57)$$
$$[\tilde{R}_j, A] = iR_{lj}, \quad [A, R_{lj}] = i\tilde{R}_j, \quad [A, S_{lj}] = 0.$$

The operators $\mathbf{R}_l$ and $\tilde{\mathbf{R}}$ are orthogonal to $\mathbf{S}_l$ in accordance with (5). Besides, $\mathbf{R}_l \cdot \tilde{\mathbf{R}} = 3X^{S_l S_r}$, and the Casimir operator is $\mathcal{K} = \mathbf{S}_l^2 + \mathbf{R}_l^2 + \tilde{\mathbf{R}}^2 + A^2 = 4$.

Like in the case of double $SO(4)$ symmetry studied above, the second step of RG procedure generates additional vertices in the exchange part of the interaction Hamiltonian (53),

$$\begin{aligned} H_{cot} &= J_1\mathbf{S}_l\cdot\mathbf{s}_l + J_2\mathbf{R}_l\cdot\mathbf{s}_l + J_3(\tilde{\mathbf{R}}_1\cdot\mathbf{s}_{rl} + \tilde{\mathbf{R}}_2\cdot\mathbf{s}_{lr}) \\ &+ J_4\mathbf{S}_l\cdot\mathbf{s}_r + J_5\tilde{\mathbf{R}}\cdot\mathbf{s}_l + J_6(\mathbf{R}_{1l}\cdot\mathbf{s}_{rl} + \mathbf{R}_{2l}\cdot\mathbf{s}_{lr}) \\ &+ J_7\mathbf{S}_l\cdot(\mathbf{s}_{lr} + \mathbf{s}_{rl}) + J_8(\tilde{\mathbf{R}}_1\cdot\mathbf{s}_{lr} + \tilde{\mathbf{R}}_2\cdot\mathbf{s}_{rl}) \\ &+ J_9\mathbf{R}_l\cdot\mathbf{s}_r + J_{10}\tilde{\mathbf{R}}\cdot\mathbf{s}_r + J_{11}\mathbf{R}_l\cdot(\mathbf{s}_{lr} + \mathbf{s}_{rl}) \\ &+ J_{12}(\mathbf{R}_{1l}\cdot\mathbf{s}_{lr} + \mathbf{R}_{2l}\cdot\mathbf{s}_{rl}), \end{aligned} \quad (58)$$

where $\mathbf{R}_{1l} = X^{S_l S_r}\tilde{\mathbf{R}}_1$, $\mathbf{R}_{2l} = \tilde{\mathbf{R}}_2 X^{S_r S_l}$. The scaling properties of the system are determined by a system of 12 scaling equations with initial conditions

$$J_1(\bar{D}) = J_l^T, \qquad J_2(\bar{D}) = J_l^{ST}, \quad (59)$$
$$J_3(\bar{D}) = \alpha_r J_{lr}, \quad J_i(\bar{D}) = 0 \quad (i = 4-12)$$

(see Eq. 36 for definitions) specifically

$$\begin{aligned} \frac{dj_1}{d\ln d} &= -\Big[j_1^2 + j_2^2 + j_5^2 + j_7^2 + j_{11}^2 + j_{11}(j_6 + j_{12}) \\ &+ \frac{j_3^2 + j_6^2 + j_8^2 + j_{12}^2}{2}\Big], \\ \frac{dj_2}{d\ln d} &= -[2(j_1 j_2 + j_7 j_{11}) + j_7(j_6 + j_{12}) - m_{lr} j_5], \\ \frac{dj_3}{d\ln d} &= -[j_3(j_1 + j_4) + j_7(j_5 + j_{10}) - m_{lr}(j_6 + j_{11})], \\ \frac{dj_4}{d\ln d} &= -\Big[j_4^2 + j_7^2 + j_9^2 + j_{10}^2 + j_{11}^2 + j_{11}(j_6 + j_{12}) \\ &+ \frac{j_3^2 + j_6^2 + j_8^2 + j_{12}^2}{2}\Big], \\ \frac{dj_5}{d\ln d} &= -[2j_1 j_5 + j_7(j_3 + j_8) - m_{lr} j_2], \\ \frac{dj_6}{d\ln d} &= -[j_6(j_1 + j_4) - m_{lr} j_3], \\ \frac{dj_7}{d\ln d} &= -\Big[\frac{(j_3 + j_8)(j_5 + j_{10}) + (j_2 + j_9)(j_6 + j_{12})}{2} \\ &+ j_7(j_1 + j_4) + j_{11}(j_2 + j_9)\Big], \\ \frac{dj_8}{d\ln d} &= -[j_8(j_1 + j_4) + j_7(j_5 + j_{10}) - m_{lr}(j_{11} + j_{12})], \\ \frac{dj_9}{d\ln d} &= -[2(j_4 j_9 + j_7 j_{11}) + j_7(j_6 + j_{12}) - m_{lr} j_{10}], \\ \frac{dj_{10}}{d\ln d} &= -[2j_4 j_{10} + j_7(j_3 + j_8) - m_{lr} j_9], \\ \frac{dj_{11}}{d\ln d} &= -[j_{11}(j_1 + j_4) + j_7(j_2 + j_9)], \\ \frac{dj_{12}}{d\ln d} &= -[j_{12}(j_1 + j_4) - m_{lr} j_8]. \end{aligned} \quad (60)$$

From equations (60), one deduces the Kondo temperature,

$$T_{K2} = \bar{D}\Big(1 - \frac{2\sqrt{2}m_{lr}}{j_1 + j_2 + \sqrt{(j_1 + j_2)^2 + 2j_3^2}}\Big)^{\frac{1}{\sqrt{2}m_{lr}}}. \quad (61)$$

Similarly to the previous case, this equation transforms into the usual exponential form when the $l-r$ symmetry of the leads is perfect,

$$\lim_{m_{lr}\to 0} T_{K2} = \bar{D}e^{-\frac{2}{j_1 + j_2 + \sqrt{(j_1 + j_2)^2 + 2j_3^2}}}. \quad (62)$$

Upon increasing m_{lr}, the symmetry reduces from $SO(5)$ to $SO(4)$. The same happens at small m_{lr} but with increasing $\bar{\delta}_l = \bar{E}_{S_l} - \bar{E}_{T_l}$. In the latter case the energy $\bar{E}_{S_l}$

is quenched, and at $\bar{\delta}_l \gg T_{K2}$ Eq. (61) transforms into $T_K = \bar{\delta}_l \exp\{-[j_1(\bar{\delta}_l) + j_3(\bar{\delta}_l)]^{-1}\}$ (cf.[14]). On the other hand, upon decreasing $\bar{\delta}_r = \bar{E}_{T_r} - \bar{E}_{S_l}$ the symmetry $P \times SO(4) \times SO(4)$ is restored at $\bar{\delta}_r < T_{K0}$. The Kondo effect disappears when $\bar{\delta}_l$ changes sign (the ground state becomes singlet).

The next asymmetric configuration is illustrated by the flow diagram of Fig.6.

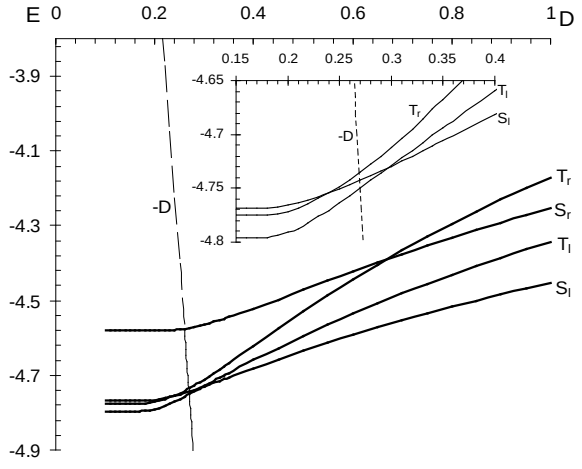

FIG. 6: Scaling trajectories for $SO(7)$ symmetry in the SW regime. Inset: Zoomed in avoided level crossing pattern near the SW line

In this case, the manifold $\{T_l, S_l, T_r\}$ is involved in the dynamical symmetry of TQD. The relevant symmetry group is $SO(7)$. It is generated by six vectors and three scalars. These are spin operators $\mathbf{S}_a$ $(a = l, r)$ and R-operator $\mathbf{R}_l$ (see Eq. 38) plus three vector operators $\tilde{\mathbf{R}}_i$ and three scalar operators A_i involving $l-r$ permutation. Here are the expressions for the spherical components of these vectors via Hubbard operators,

$$\begin{aligned}
\tilde{R}_1^+ &= \sqrt{2}(X^{1_r 0_l} + X^{0_l \bar{1}_r}), \quad \tilde{R}_1^z = X^{1_l 1_r} - X^{\bar{1}_r \bar{1}_l}, \\
\tilde{R}_2^+ &= \sqrt{2}(X^{1_l 0_r} + X^{0_r \bar{1}_l}), \quad \tilde{R}_2^z = X^{1_r 1_l} - X^{\bar{1}_l \bar{1}_r}, \\
\tilde{R}_3^+ &= \sqrt{2}(X^{1_r S_l} - X^{S_l \bar{1}_r}), \quad \tilde{R}_3^z = -(X^{0_r S_l} + X^{S_l 0_r}).
\end{aligned} \tag{63}$$

The scalar operators A_1, A_2, A_3 now involve the $l - r$ permutations for the triplet states. They are defined as

$$\begin{aligned}
A_1 &= \frac{i\sqrt{2}}{2}\left(X^{1_r \bar{1}_l} - X^{1_l \bar{1}_r + X^{\bar{1}_r 1_l} - X^{\bar{1}_l 1_r}}\right), \\
A_2 &= \frac{\sqrt{2}}{2}\left(X^{1_l \bar{1}_r} - X^{1_r \bar{1}_l} + X^{\bar{1}_r 1_l} - X^{\bar{1}_l 1_r}\right), \\
A_3 &= i\left(X^{0_l 0_r} - X^{0_r 0_l}\right).
\end{aligned} \tag{64}$$

The (somewhat involved) commutation relations of o_7 algebra for these operators and various kinematic constraints are presented in Appendix D. The SW transformation results in the effective cotunneling Hamiltonian

$$\begin{aligned}
H_{cot} &= \sum_{\Lambda = T_l, S_l, T_r} \bar{E}_\Lambda X^{\Lambda\Lambda} + M_{lr}(X^{T_l T_r} + X^{T_r T_l}) \\
&+ \sum_{k\sigma} \sum_{a=l,r} \epsilon_{ka} c^+_{ak\sigma} c_{ak\sigma} + t_{lr} \sum_{k\sigma} \sum_{a=l,r} c^+_{ak\sigma} c_{\bar{a}k\sigma} \\
&+ \sum_{a=l,r} J_{1a} \mathbf{S}_a \cdot \mathbf{s}_a + J_2 \sum_{a=l,r} \mathbf{S}_{a\bar{a}} \cdot \mathbf{s}_{a\bar{a}} \\
&+ J_3(\tilde{\mathbf{R}}_3^{(1)} \cdot \mathbf{s}_{rl} + \tilde{\mathbf{R}}_3^{(2)} \cdot \mathbf{s}_{lr}) + J_4 \mathbf{R}_l \cdot \mathbf{s}_l,
\end{aligned} \tag{65}$$

where $J_{1a} = J_a^T$, $J_2 = J_{lr}$, $J_3 = \alpha_l J_{lr}$, $J_4 = \alpha_l J_l^T$ and $\mathbf{S}_{a\bar{a}} = \sum_\mu X^{\mu_a \mu_{\bar{a}}} \mathbf{S}_{\bar{a}}$. The spherical components of the vector operators $\tilde{\mathbf{R}}_1$ and $\tilde{\mathbf{R}}_2$ are

$$\begin{aligned}
\tilde{R}_3^{(1)+} &= \sqrt{2} X^{1_r S_l}, \quad \tilde{R}_3^{(1)-} = -\sqrt{2} X^{\bar{1}_r S_l}, \\
\tilde{R}_3^{(2)+} &= (\tilde{R}_3^{(1)-})^\dagger, \quad \tilde{R}_3^{(2)-} = (\tilde{R}_3^{(1)+})^\dagger, \\
\tilde{R}_{3z}^{(1)} &= -X^{0_r S_l}, \quad \tilde{R}_{3z}^{(2)} = (\tilde{R}_{3z}^{(1)})^\dagger.
\end{aligned} \tag{66}$$

It is easy to see that $\mathbf{S}_{lr} + \mathbf{S}_{rl} = \tilde{\mathbf{R}}_1 + \tilde{\mathbf{R}}_2$ and $\tilde{\mathbf{R}}_3 = \tilde{\mathbf{R}}_3^{(1)} + \tilde{\mathbf{R}}_3^{(2)}$.

Like in the case of $SO(5)$ symmetry, the tunneling terms $M_{lr} X^{T_a T_{\bar{a}}}$ generate additional vertices in the renormalized Hamiltonian H_{cot}. The number of these vertices and the corresponding scaling equations is too wide to be presented here. We leave the description of RG procedure for $SO(7)$ group for the next section (as well as the case of TQD with odd occupation), where the case of $M_{lr} = 0$ is considered. In that case the scaling equations describing the Kondo physics of TQD with $SO(n)$ symmetry are more compact.

B. Section summary

The basic physics for all $SO(n)$ symmetries is the same, and we summarize it here. We have analyzed several examples of TQD with even occupation in the parallel geometry (Fig. 1). Our analysis demonstrates the principal features of Kondo effect in CQD in comparison with the conventional SQD composed of a single well. These examples teach us that in Kondo tunneling through CQD, not only the spin rotation but also the "Runge-Lenz" type operators $\mathbf{R}$ and $\tilde{\mathbf{R}}$ are involved. Physically, the operators $\tilde{\mathbf{R}}$ describe left-right transitions, and different Young schemes give different spin operators in the effective co-tunneling Hamiltonians (see Appendix E).

IV. TRIPLE QUANTUM DOT IN SERIES

A. Motivation

It was mentioned already in Section III that a TQD with leads possessing perfect $l - r$ symmetry can be mapped onto a TQD in a series by means of geometrical

conformal transformation. Indeed, if the inter-channel tunneling amplitude t_{lr} in the Hamiltonian (24) is zero, one may apply the rotation in the source-drain space separately to each channel and exclude the odd $s-d$ combination of lead states both in the l- and r-channel.[11] Since now each lead is coupled to its own reservoir, and one arrives at the series configuration shown in Fig.7.

It is virtually impossible to conceive an additional transformation after which the odd combination of lead states are excluded from the tunneling Hamiltonian[28]. As a result, the challenging situation arises in case of odd occupation $N=3$, where the net spin of TQD is $S=1/2$, and the two leads play part of two channels in Kondo tunneling Hamiltonian. Unfortunately, despite the occurrence of two electron channels in the spin Hamiltonian, the complete mapping on the two-channel Kondo problem is not attained because there is an additional cotunneling term $J_{lr}\mathbf{S}\cdot\mathbf{s}_{lr}+H.c.$ ($\mathbf{s}_{lr}$ is determined by (39)) which turns out to be relevant, and the two-channel fixed point cannot be reached. And yet, from the point of view of dynamical symmetry the series geometry offers a new perspective which we analyze in the present section for cases of even and odd occupation.

B. Even occupation

Consider then a TQD in series (Fig.7) with four electron occupation $N=4$. The Hamiltonian of the system can be written in the form,

$$\begin{aligned} H &= \sum_{\Lambda_a} E_{\Lambda_a} X^{\Lambda_a\Lambda_a} + \sum_{\lambda} E_\lambda X^{\lambda\lambda} + \sum_{k\sigma}\sum_{b=s,d} \epsilon_{kb} c^+_{bk\sigma} c_{bk\sigma} \\ &+ \sum_{\Lambda\lambda}\sum_{k\sigma} [(V^{\lambda\Lambda}_{l\sigma} c^+_{sk\sigma} + V^{\lambda\Lambda}_{r\sigma} c^+_{dk\sigma}) X^{\lambda\Lambda} + H.c.]. \end{aligned} \quad (67)$$

Here $|\Lambda\rangle$, $|\lambda\rangle$ are the four- and three-electron eigenfunctions (A5) and (A9), respectively; E_Λ, E_λ are the four- and three-electron energy levels, respectively; $X^{\lambda\lambda'}=|\lambda\rangle\langle\Lambda|$ are number changing dot Hubbard operators. The tunneling amplitudes $V^{\lambda\Lambda}_{a\sigma}=V_a\langle\lambda|d_{a\sigma}|\Lambda\rangle$ $(a=l,r)$ depend explicitly on the respective $3-4$ particle quantum numbers λ, Λ. Note that direct tunneling through the TQD is suppressed due to electron level mismatch and Coulomb blockade, so that only *cotunneling* mechanism contributes to the current.

The generic Hamiltonian (35) simplifies in this case to

$$\begin{aligned} H_{cot} &= \sum_{\Lambda_a} \bar{E}_{\Lambda_a} X^{\Lambda_a\Lambda_a} + \sum_{k\sigma}\sum_{b=l,r} \epsilon_{kb} c^\dagger_{bk\sigma} c_{bk\sigma} \\ &+ \sum_{a=l,r} J^T_a \mathbf{S}_a\cdot\mathbf{s}_a + J_{lr}\hat{P}\sum_{a=l,r}\mathbf{S}_a\cdot\mathbf{s}_{\bar{a}a} \\ &+ \sum_{a=l,r} J^{ST}_a \mathbf{R}_a\cdot\mathbf{s}_a + J_{lr}\sum_{a=l,r}\tilde{\mathbf{R}}_a\cdot\mathbf{s}_{a\bar{a}}, \end{aligned} \quad (68)$$

(the notation l,r is used for the electron states both in the leads and in the TQD). The antiferromagnetic coupling constants are defined by (36). The vectors $\mathbf{S}_a$, $\mathbf{R}_a$ and $\tilde{\mathbf{R}}_a$ are the dot operators (38), $\hat{P}$ is the permutation operator (37), and the components of the vectors $\mathbf{s}_a$, $\mathbf{s}_{a\bar{a}}$ are determined in Eqs. (20) (with $\alpha=a=l,r$) and (39). The vector operators $\mathbf{S}_a$, $\mathbf{R}_a$, $\tilde{\mathbf{R}}_a$ and the permutation operator $\hat{P}$ manifest the dynamical symmetry of the TQD.

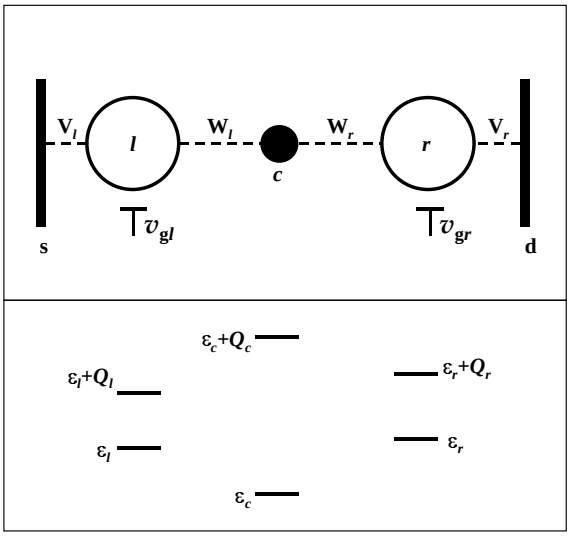

FIG. 7: Triple quantum dot in series. Left (l) and right (r) dots are coupled by tunneling $W_{l,r}$ to the central (c) dot and by tunneling $V_{l,r}$ to the source (s) (left) and drain (d) (right) leads.

We now discuss possible realization of $P\times SO(4)\times SO(4)$, $SO(5)$ and $SO(7)$ symmetries arising in the TQD with $N=4$. Due to the absence of interchannel mixing, the avoided crossing effect does not arise in the series geometry. As a result, all cases of high symmetry are characterized by the same flow diagram of Figs. 3,5 and 6 but *without avoided crossing effects shown in the insets.*

Let us commence the analysis of the Kondo effect in the series geometry with the case $P\times SO(4)\times SO(4)$ where $E_{lc}=E_{rc}$ and $\Gamma_{T_r}=\Gamma_{T_l}$ (Fig.3). In this case the exchange part of the Hamiltonian (68) is a simplified version of the Hamiltonian (46) with the boundary conditions (47). The scaling equations are the same as (48) with $m_{lr}=0$. Solving them one gets Eq.(50) for the Kondo temperature.

When $\bar{E}_{S_l}\approx\bar{E}_{T_l}\approx\bar{E}_{S_r}<\bar{E}_{T_r}$ (Fig.5), the TQD possesses the $SO(5)$ symmetry. In this case the interaction Hamiltonian has the form

$$H_{cot}=J_1\mathbf{S}_l\cdot\mathbf{s}_l+J_2\mathbf{R}_l\cdot\mathbf{s}_l+J_3(\tilde{\mathbf{R}}_1\cdot\mathbf{s}_{rl}+\tilde{\mathbf{R}}_2\cdot\mathbf{s}_{lr}), \quad (69)$$

which is the same as in Eq.(53) with $\tilde{\mathbf{R}}_1$, $\tilde{\mathbf{R}}_2$ determined by Eq.(54). Respectively, the effective Hamiltonian for the Anderson scaling is a reduced version of the Hamiltonian (58)

$$\begin{aligned} H_{cot} &= J_1\mathbf{S}_l\cdot\mathbf{s}_l+J_2\mathbf{R}_l\cdot\mathbf{s}_l \\ &+ J_3(\tilde{\mathbf{R}}_1\cdot\mathbf{s}_{rl}+\tilde{\mathbf{R}}_2\cdot\mathbf{s}_{lr})+J_4\mathbf{S}_l\cdot\mathbf{s}_r, \end{aligned} \quad (70)$$

with the boundary conditions (59) for J_i, $i=1-4$.

The scaling equations have the form

$$\begin{aligned}\frac{dj_1}{d\ln d} &= -\left[j_1^2+j_2^2+\frac{j_3^2}{2}\right],\\ \frac{dj_2}{d\ln d} &= -2j_1j_2,\\ \frac{dj_3}{d\ln d} &= -j_3(j_1+j_4),\\ \frac{dj_4}{d\ln d} &= -\left[j_4^2+\frac{j_3^2}{2}\right].\end{aligned} \tag{71}$$

Of course, Eqs.(71) for the Kondo temperature yield the limiting value (62).

When $\bar{E}_{T_l}\approx\bar{E}_{T_r}<\bar{E}_{S_l},\bar{E}_{S_r}$ (Fig.6), the TQD possesses the $SO(7)$ symmetry. In this case the Anderson RG procedure adds three additional vertices in the exchange part of the basic SW Hamiltonian (65),

$$\begin{aligned}H_{cot} &= \sum_{a=l,r}J_{1a}\mathbf{S}_a\cdot\mathbf{s}_a+J_2\sum_{a=l,r}\mathbf{S}_{a\bar{a}}\cdot\mathbf{s}_{a\bar{a}}\\ &+ J_3(\tilde{\mathbf{R}}_3^{(1)}\cdot\mathbf{s}_{rl}+\tilde{\mathbf{R}}_3^{(2)}\cdot\mathbf{s}_{lr})+J_4\mathbf{R}_l\cdot\mathbf{s}_l\\ &+ \sum_{a=l,r}J_{5a}\mathbf{S}_a\cdot\mathbf{s}_{\bar{a}}+J_6\mathbf{R}_l\cdot\mathbf{s}_r.\end{aligned} \tag{72}$$

The boundary conditions for solving the scaling equations are

$$\begin{aligned}&J_{1a}(\bar{D})=J_a^T,\quad J_2(\bar{D})=J_{lr},\quad J_3(\bar{D})=\alpha_lJ_{lr},\\ &J_4(\bar{D})=\alpha_lJ_l^T,\quad J_{5a}(\bar{D})=J_6(\bar{D})=0\ (a=l,r).\end{aligned} \tag{73}$$

The system of scaling equations

$$\begin{aligned}\frac{dj_{1l}}{d\ln d} &= -\left[j_{1l}^2+\frac{j_2^2}{2}+j_4^2\right],\\ \frac{dj_{1r}}{d\ln d} &= -\left[j_{1r}^2+\frac{j_2^2}{2}+\frac{j_3^2}{2}\right],\\ \frac{dj_2}{d\ln d} &= -\frac{j_2(j_{1l}+j_{1r}+j_{5l}+j_{5r})+j_3(j_4+j_6)}{2},\\ \frac{dj_3}{d\ln d} &= -\left[j_2(j_4+j_6)+j_3(j_{1r}+j_{5r})\right],\\ \frac{dj_4}{d\ln d} &= -\left[2j_{1l}j_4+j_2j_3\right],\\ \frac{dj_{5l}}{d\ln d} &= -\left[j_{5l}^2+\frac{j_2^2}{2}+j_6^2\right],\\ \frac{dj_{5r}}{d\ln d} &= -\left[j_{5r}^2+\frac{j_2^2}{2}+\frac{j_3^2}{2}\right],\\ \frac{dj_6}{d\ln d} &= -\left[2j_{5l}j_6+j_2j_3\right]\end{aligned} \tag{74}$$

is now solvable analytically, and the Kondo temperature is,

$$T_K=\bar{D}\exp\left\{\frac{4}{2j_++\sqrt{4j_-^2+3(j_2+j_3)^2}}\right\}, \tag{75}$$

where $j_+=j_{1l}+j_4+j_{1r}$, $j_-=j_{1l}+j_4-j_{1r}$.

Like in the cases considered above, the Kondo temperature and the dynamical symmetry itself depend on the level splitting. On quenching the S_l state (increasing $\bar{\delta}_{lr}=\bar{E}_{S_l}-\bar{E}_{T_r}$), the pattern is changed into a $P\times SO(3)\times SO(3)$ symmetry of two degenerate triplets with a mirror reflection axis. Changing the sign of δ_{lr} one arrives at a singlet regime with $T_K=0$.

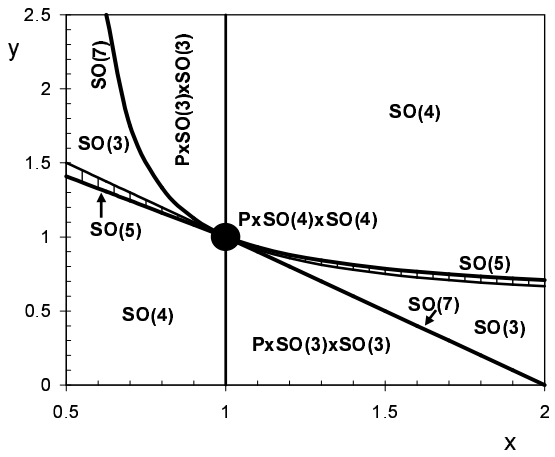

FIG. 8: Phase diagram of TQD. The numerous dynamical symmetries of a TQD in the parallel geometry are presented in the plane of experimentally tunable parameters $x=\Gamma_l/\Gamma_r$ and $y=E_{lc}/E_{rc}$.

The results of calculations described in this subsection are summarized in Fig.8. The central domain of size T_{K0} describes the fully symmetric state where there is left-right symmetry. Other regimes of Kondo tunneling correspond to lines or segments in the $\{x,y\}$ plane. These lines correspond to cases of higher conductance (ZBA). On the other hand, at some regions, the TQD has a singlet ground state and the Kondo effect is absent. These are marked by the vertically hatched domain. Both the tunneling rates which enter the ratio x and the relative level positions which determine the parameter y depend on the applied potentials, so the phase diagram presented in Fig.8 can be scanned *experimentally* by appropriate variations of V_a and v_{ga}. This is a rare occasion where an abstract concept like dynamical symmetry can be felt and tuned by experimentalists. The quantity that is measured in tunneling experiments is the zero-bias anomaly (ZBA) in tunnel conductance g.[9] The ZBA peak is strongly temperature dependent, and this dependence is scaled by T_K. In particular, in a high temperature region $T>T_K$, where the scaling approach is valid, the conductance behaves as

$$g(T)\sim\ln^{-2}(T/T_K). \tag{76}$$

As it has been demonstrated above, T_K in CQD is a non-universal quantity due to partial break-down of dynamical symmetry in these quantum dots. It has a maximum value in the point of highest symmetry

$P \times SO(4) \times SO(4)$, and depends on the parameters δ_a in the less symmetric phases (see, e.g., Eqs. 50, 52, 62, 75). Thus, scanning the phase diagram means changing $T_K(\delta_a)$. These changes are shown in Fig.9 which

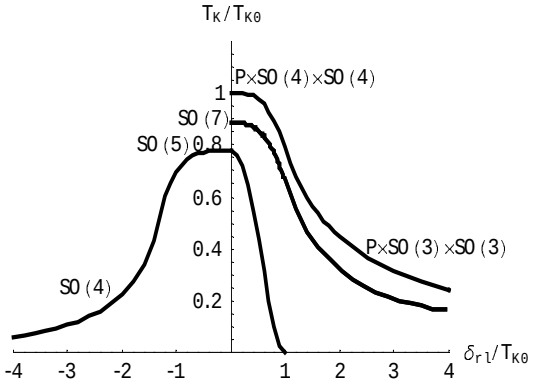

FIG. 9: Variation of Kondo temperature with $\delta_{rl} \equiv v_{gr} - v_{gl}$. Increasing this parameter removes some of the degeneracy and either "breaks" or reduces the corresponding dynamical symmetry.

illustrates the evolution of T_K with δ_{rl} for $x = 0.96$, 0.8 and 0.7 corresponding to a symmetry change from $P \times SO(4) \times SO(4)$, $SO(7)$ to $P \times SO(3) \times SO(3)$ and from $SO(5)$ to $SO(4)$, respectively. It is clear that the conductance measured at given T should follow variation of T_K in accordance with (76).

C. Odd occupation

We now turn our attention to investigation of the dynamical symmetries of TQD in series with odd occupation $N = 3$, whose low-energy spin multiplet contains two spin 1/2 doublets $|B_{1,2}\rangle$ and a spin quartet $|Q\rangle$,

$$\begin{aligned} E_{B_1} &= \varepsilon_c + \varepsilon_l + \varepsilon_r - \frac{3}{2}\left[W_l\beta_l + W_r\beta_r\right], \\ E_{B_2} &= \varepsilon_c + \varepsilon_l + \varepsilon_r - \frac{1}{2}\left[W_l\beta_l + W_r\beta_r\right], \\ E_Q &= \varepsilon_c + \varepsilon_l + \varepsilon_r. \end{aligned} \tag{77}$$

There are also four charge-transfer excitonic counterparts of the spin doublets separated by the charge transfer gaps $\sim \varepsilon_l - \varepsilon_c + Q_l$ and $\varepsilon_r - \varepsilon_c + Q_r$ from the above states (see Appendix A).

Like in the four-electron case, the scaling equations (31) may be derived with different tunneling rates for different spin states (Γ_Q for the quartet and $\Gamma_{B_i} (i = 1, 2)$ for the doublets).

$$\begin{aligned} &\Gamma_Q = \pi\rho_0 \left(V_l^2 + V_r^2\right), \\ &\Gamma_{B_1} = \gamma_1^2\Gamma_Q, \quad \Gamma_{B_2} = \gamma_2^2\Gamma_Q, \end{aligned} \tag{78}$$

with

$$\gamma_1 = \sqrt{1 - \frac{3}{2}\left(\beta_l^2 + \beta_r^2\right)}, \quad \gamma_2 = \sqrt{1 - \frac{1}{2}\left(\beta_l^2 + \beta_r^2\right)}. \tag{79}$$

Since $\Gamma_Q > \Gamma_{B_1}, \Gamma_{B_2}$, the scaling trajectories cross in a unique manner: This is the complete degenerate configuration where all three phase trajectories E_Λ intersect $[E_Q(D^\star) = E_{B1}(D^\star) = E_{B2}(D^\star)]$ at the same point $D^\star$. This happens at bandwidth $D = D^\star$ (Fig.10) whose value is estimated as

$$D^\star = D_0 \exp\left(-\frac{\pi r}{\Gamma_Q}\right), \tag{80}$$

where

$$r = \frac{W_l^2 E_{rc} + W_r^2 E_{lc}}{W_l^2 E_{rc}^2 + W_r^2 E_{lc}^2} E_{lc} E_{rc}.$$

If this degenerate point occurs in the SW crossover re-

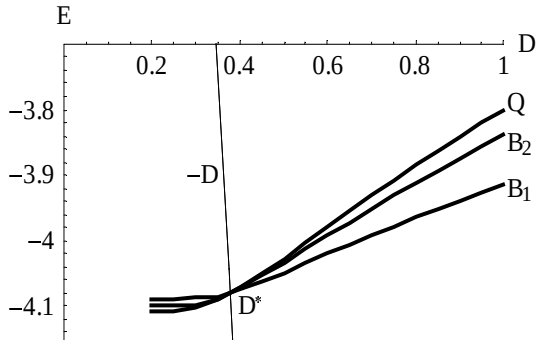

FIG. 10: Scaling trajectories resulting in $SO(4) \times SU(2)$ symmetry of TQD with $N = 3$.

gion, i.e., if $D^\star \approx \bar{D}$, the SW procedure involves all three spin states, and it results in the following cotunneling Hamiltonian

$$H_{cot} = \sum_{a=l,r} \left(J_a^T \mathbf{S} + J_a^{ST} \mathbf{R}\right) \cdot \mathbf{s}_a, \tag{81}$$

where $\mathbf{S}$ is the spin 1 operator and $\mathbf{R}$ is the R-operator describing S/T transition similar to that for spin rotator[13]. The coupling constants are

$$J_a^T = \frac{4\gamma_1 |V_a|^2}{3(\epsilon_F - \varepsilon_a)}, \quad J_a^{ST} = \gamma_2 J_{lr}^T. \tag{82}$$

This is a somewhat unexpected situation where Kondo tunneling in a quantum dot with *odd* occupation demonstrates the exchange Hamiltonian of a quantum dot with *even* occupation. The reason for this scenario is the specific structure of the wave function of TQD with $N = 3$. The corresponding wave functions $|\Lambda\rangle$ (see Appendix A) are vector sums of states composed of a "passive" electron sitting in the central dot and singlet/triplet (S/T) two-electron states in the l, r dots. Constructing the eigenstates $|\Lambda\rangle$ using certain Young tableaux (see Appendix D), one concludes that the spin dynamics of such TQD is represented by the spin 1 operator $\mathbf{S}$ corresponding to the $l-r$ triplet, the corresponding R-operator $\mathbf{R}$ and the spin 1/2 operator $\mathbf{s}_c$ of a passive electron in the central

well. The latter does not enter the effective Hamiltonian H_{cot} (81) but influences the kinematic constraint via Casimir operator $\mathcal{K} = \mathbf{S}^2 + \mathbf{M}^2 + \mathbf{s}_c^2 = \frac{15}{4}$. The dynamical symmetry is therefore $SO(4) \times SU(2)$, and only the $SO(4)$ subgroup is involved in Kondo tunneling.

The scaling equations have the form,

$$\begin{aligned} \frac{dj_{1a}}{d\ln d} &= -[j_{1a}^2 + j_{2a}^2], \\ \frac{dj_{2a}}{d\ln d} &= -2j_{1a}j_{2a}, \end{aligned} \tag{83}$$

where $j_{1a} = \rho_0 J_a^T$, $j_{2a} = \rho_0 J_a^{ST}$ $(a = l, r)$. From Eqs. (83) we obtain the Kondo temperature,

$$T_K = \max\{\mathrm{T_{Kl}}, \mathrm{T_{Kr}}\}, \tag{84}$$

with $T_{Ka} = \bar{D}\exp\left[-1/(j_{1a} + j_{2a})\right]$.

An additional dynamical symmetry arises in the case when $D^\star > \bar{D}$. In this case the ground state of TQD is a quartet S=3/2, and we arrive at a standard underscreened Kondo effect for $SU(2)$ quantum dot as an ultimate limit of the above highly degenerate state.

D. Section summary

To conclude this section, it might be useful here to underscore the following points: 1) The difference between series and parallel geometries of TQD coupled to the leads by two channels exists only at non-zero interchannel mixing in the leads, $t_{lr} \neq 0$. 2) One may control the dynamical symmetry of Kondo tunneling through TQD by varying the gate voltage and/or lead-dot tunneling rate. 3) In the case of odd electron occupation ($N = 3$) when the ground-state of the isolated TQD is a doublet and higher spin excitations can be neglected, the effective low-energy Hamiltonian of a TQD in series manifests a two-channel Kondo problem albeit *only in the weak coupling regime*.[28] To describe the flow diagram in this case, one should go beyond the one-loop approximation in RG flow equations.[30] 4) The nominal spin of CQD does not necessarily coincide with that involved in Kondo tunneling. A simple albeit striking realization of this scenario in this context is the case of TQD with $N = 3$, which manifests itself as a dot with integer or half-integer spin depending on gate voltages.

V. ANISOTROPIC KONDO TUNNELING THROUGH TQD IN SERIES GEOMETRY

A. Generalities

In all examples of CQDs considered in the previous sections the co-tunneling problem is mapped on the specific spin Hamiltonian where both $\mathbf{S}$ and $\mathbf{R}$ vectors are involved in resonance cotunneling. There are, however, more exotic situations where the effective spin Hamiltonian is in fact a "Runge-Lenz" Hamiltonian in the sense that the vectors $\mathbf{R}$ *alone* are responsible for Kondo effect. Actually, just this aspect of dynamical symmetry in Kondo tunneling was considered in the theoretical papers cited in Ref. 6 and observed experimentally in Ref. 25, in which the Kondo effect in planar and vertical QDs induced by external magnetic field B has been observed. In this section we lay down the theoretical basis for this somewhat unusual kind of Kondo effect.

Consider again the case of TQD in series geometry with $N = 4$. In the previous sections the variation of spin symmetry is due to the interplay of two contributions to indirect exchange coupling between the spins $\mathbf{S}_a$. One source of such an exchange is tunneling within the CQD (amplitudes W_a) and another one is the tunneling between the dots and the leads (amplitudes V_a). An appropriate tuning of these two contributions results in occasional degeneracy of spin states (elimination of exchange splitting), and various combinations of these occasional degeneracies lead to the rich phase diagram presented in Fig. 8. A somewhat more crude approach, yet more compliant with experimental observation of such interplay is provided by the Zeeman effect. This mechanism is effective for CQD which remains in a singlet ground state after all exchange renormalizations have taken place. The negative exchange energy δ_a may then be compensated by the Zeeman splitting of the nearest triplet states, and Kondo effect arises once this compensation is complete.[6] From the point of view of dynamical symmetry, the degeneracy induced by magnetic field means realization of one possible subgroup of the non-compact group $SO(n)$ (see Eq. 21 and corresponding discussion in Section II). The transformation $SO(4) \to SU(2)$ for DQD in magnetic field was discussed in Ref. 13.

B. Quantum dot with SU(3) dynamical symmetry

In similarity with DQD, the Kondo tunneling may be induced by external field B in the non-magnetic sector of the phase diagram of Fig. 8. A very peculiar Kondo tunneling is induced by an external magnetic field B in the non-magnetic sector of the phase diagram of Fig. 8 close to the $SO(5)$ line. In this case, a remarkable symmetry reduction occurs when the Zeeman splitting compensates negative $\delta_{l,r} = E_{S_l,r} - E_{T_l}$. Then we are left in the subspace of states $\{T1_l, S_l, S_r\}$, and the interaction Hamiltonian has the form,

$$\begin{aligned} \widetilde{H}_{cot} &= (J_1 R_1^z + J_2 R_2^z) s_l^z + \frac{\sqrt{2}}{2} J_{3l} \left(R_1^+ s_l^- + R_1^- s_l^+\right) \\ &+ \frac{\sqrt{2}}{2} J_{3r} (R_2^+ s_{lr}^- + R_2^- s_{rl}^+) + J_4 \left(R_3 s_{lr}^z + R_4 s_{rl}^z\right) \\ &+ (J_5 R_1^z + J_6 R_2^z) s_r^z + J_7 (R_1^+ s_r^- + R_1^- s_r^+). \end{aligned} \tag{85}$$

Here

$$J_1(\bar{D}) = J_2(\bar{D}) = \frac{2J_l^T}{3}, \quad J_{3l}(\bar{D}) = J_l^{ST},$$
$$J_{3r}(\bar{D}) = \alpha_r J_{lr}, \quad J_i(\bar{D}) = 0 \ \ (i = 4-7). \quad (86)$$

The operators $\mathbf{R}_1$, $\mathbf{R}_2$, R_3 and R_4 are defined as,

$$R_1^z = \frac{1}{2}(X^{1_l 1_l} - X^{S_l S_l}), \ R_1^+ = X^{1_l S_l}, \ R_1^- = (R_1^+)^\dagger,$$
$$R_2^z = \frac{1}{2}(X^{1_l 1_l} - X^{S_r S_r}), \ R_2^+ = X^{1_l S_r}, \ R_2^- = (R_2^+)^\dagger,$$
$$R_3 = \frac{\sqrt{3}}{2} X^{S_l S_r}, \qquad R_4 = \frac{\sqrt{3}}{2} X^{S_r S_l}. \quad (87)$$

We see that the anisotropic Kondo Hamiltonian (85) is quite unconventional. There are several different terms responsible for transverse and longitudinal exchange involving the R-operators which generate both S_a/T and $S_a/S_{\bar{a}}$ transitions.

The operators (87) obey the following commutation relations,

$$[R_{1j}, R_{1k}] = ie_{jkm}R_{1m}, \qquad [R_{2j}, R_{2k}] = ie_{jkm}R_{2m},$$
$$[R_{1j}, R_{2k}] = \frac{\sqrt{3}}{6}(R_3 - R_4)\delta_{jk}(1-\delta_{jz})$$
$$+\frac{i}{2}e_{jkm}\Big(R_{1m}\delta_{kz} + R_{2m}\delta_{jz} - \frac{\sqrt{3}}{3}\delta_{mz}(R_3+R_4)\Big),$$
$$[R_{1j}, R_3] = -\frac{1}{2}R_3\delta_{jz} + \frac{\sqrt{3}}{4}(R_{2x} + iR_{2y})(\delta_{jx} - i\delta_{jy}),$$
$$[R_{1j}, R_4] = \frac{1}{2}R_4\delta_{jz} - \frac{\sqrt{3}}{4}(R_{2x} - iR_{2y})(\delta_{jx} + i\delta_{jy}),$$
$$[R_{2j}, R_3] = \frac{1}{2}R_3\delta_{jz} - \frac{\sqrt{3}}{4}(R_{1x} + iR_{1y})(\delta_{jx} + i\delta_{jy}),$$
$$[R_{2j}, R_4] = -\frac{1}{2}R_4\delta_{jz} + \frac{\sqrt{3}}{4}(R_{1x} + iR_{1y})(\delta_{jx} - i\delta_{jy}),$$
$$[R_3, R_4] = \frac{3}{2}(R_2^z - R_1^z). \quad (88)$$

These operators generate the algebra u_3 in the reduced spin space $\{T1_l, S_l, S_r\}$ specified by the Casimir operator

$$\mathbf{R}_1^2 + \mathbf{R}_2^2 + R_3^2 + R_4^2 = \frac{3}{2}.$$

Therefore, in this case the TQD possesses $SU(3)$ symmetry. These R operators may be represented via the familiar Gell-Mann matrices λ_i $(i = 1, ..., 8)$ for the $SU(3)$ group,

$$R_1^+ = \frac{1}{2}(\lambda_1 + i\lambda_2), \qquad R_1^- = \frac{1}{2}(\lambda_1 - i\lambda_2),$$
$$R_1^z = \frac{\lambda_3}{2}, \qquad R_2^z = \frac{1}{4}(\lambda_3 + \sqrt{3}\lambda_8),$$
$$R_2^+ = \frac{1}{2}(\lambda_4 + i\lambda_5), \qquad R_2^- = \frac{1}{2}(\lambda_4 - i\lambda_5),$$
$$R_3 = \frac{\sqrt{3}}{4}(\lambda_6 + i\lambda_7), \quad R_4 = \frac{\sqrt{3}}{4}(\lambda_6 - i\lambda_7).$$

As far as the RG procedure for the "Runge-Lenz" exchange Hamiltonian (85) the poor-man scaling procedure is applicable also for the R operators. The scaling equations have the form,

$$\frac{dj_1}{d\ln d} = -2j_{3l}^2, \qquad \frac{dj_2}{d\ln d} = -j_{3r}^2,$$
$$\frac{dj_{3l}}{d\ln d} = -\Big[j_{3l}\Big(j_1 + \frac{j_2}{2}\Big) - \frac{\sqrt{3}}{4}j_{3r}j_4\Big],$$
$$\frac{dj_{3r}}{d\ln d} = -\frac{j_{3r}(j_1 + 2j_2 + j_5 + 2j_6) - \sqrt{3}j_4(j_{3l} + \sqrt{2}j_7)}{4},$$
$$\frac{dj_4}{d\ln d} = j_{3r}\Big(\frac{\sqrt{3}}{3}j_{3l} + \frac{\sqrt{2}}{2}j_7\Big),$$
$$\frac{dj_5}{d\ln d} = -4j_7^2, \qquad \frac{dj_6}{d\ln d} = -j_{3r}^2,$$
$$\frac{dj_7}{d\ln d} = -\Big[j_5j_7 + \frac{j_6j_7}{2} - \frac{\sqrt{6}}{8}j_{3r}j_4\Big], \quad (89)$$

where $j = \rho_0 J$. We cannot demonstrate analytical solution of this system, but the numerical solution shows that stable infinite fixed point exists in this case like in all previous configurations.

Another type of field induced Kondo effect is realized in the symmetric case of $\delta = E_{S_g} - E_{T_{g,u}} < 0$. Now the Zeeman splitting compensates negative δ. Then the two components of the triplets, namely $E_{T1_{g,u}}$ cross with the singlet state energy E_{S_g}, and the symmetry group of the TQD in magnetic field is $SU(3)$ as in the case considered above.

C. Section summary

It has been demonstrated that the loss of rotational invariance in external magnetic field radically changes the dynamical symmetry of TQD. We considered here two examples of symmetry reduction, namely $SO(5) \to SU(3)$ and $P \times SO(4) \times SO(4) \to SU(3)$. In all cases the Kondo exchange is anisotropic, which, of course, reflects the axial anisotropy induced by the external field. These examples as well as the $SO(4) \to SU(2)$ reduction considered earlier[12,13] describe the magnetic field induced Kondo effect owing to the dynamical symmetry of complex quantum dots. Similar reduction $SO(n) \to SU(n')$ induced by magnetic field may arise also in more complicated configurations, and in particular in the parallel geometry. The immense complexity of scaling procedure adds nothing new to the general pattern of the field induced anisotropy of Kondo tunneling, so we confine ourselves with these two examples .

Although the anisotropic Kondo Hamiltonian was introduced formally at the early stage of Kondo physics[31], it was rather difficult to perceive how such Hamiltonian is derivable from the generic Anderson-type Hamiltonian. It was found that the effective anisotropy arises in cases where the pseudo-spin degrees of freedom (like a two-level system) are responsible for anomalous scattering. Another possibility is the introduction of mag-

netic anisotropy in the generic spin Hamiltonian due to spin-orbit interaction (see Ref. 32 for a review of such models). One should also mention the remarkable possibility of magnetic field induced anisotropic Kondo effect on a magnetic impurity in ferromagnetic rare-earth metals with easy plane magnetic anisotropy.[33] This model is close to our model from the point of view of effective spin Hamiltonian, but the sources of anisotropy are different in the two systems. In our case the interplay between singlet and triplet components of spin multiplet is an eventual source both of Kondo effect itself and of its anisotropy in external magnetic field. Previously, the manifestation of $SU(3)$ symmetry in anisotropic magnetic systems were established in Ref.[34]. It was shown, in particular, that this dynamical symmetry predetermines the properties of collective excitations in anisotropic Heisenberg ferromagnet. In the presence of single-ion anisotropy the relation between the Hubbard operators for $S = 1$ and Gell-Mann matrices λ were established. It worth also mentioning in this context the $SU(4) \supset SO(5)$ algebraic structure of superconducting and antiferromagnetic coherent states in cuprate High-T_c materials[35].

VI. CONCLUSIONS

We have analyzed the occurrence of dynamical symmetries in complex quantum dots. These symmetries emerge when the dot is coupled with metallic electrodes under the conditions of strong Coulomb blockade and nearly degenerate low energy spin spectrum. It can be achieved either by an application of an external magnetic field or due to dot-lead tunneling which, as we have seen, results in level renormalization and the emergence of an additional symmetry. Although the main focus in this paper is related to the study of triple quantum dots, the generalization to other quantum dot structures is indeed straightforward.

Since we were interested in a symmetry aspect of Kondo tunneling Hamiltonian, we restricted ourselves by derivation of RG flow equations and solving them for obtaining the Kondo temperature. In all cases the TQDs possess strong coupling fixed point characteristic for spin 1/2 and/or spin 1 case. We did not calculate the tunnel conductance in details, because it reproduces the main features of Kondo-type zero bias anomalies studied extensively by many authors (see, e.g.,[6,11,12,13,14,21,22]). The novel feature is the possibility of changing T_K by scanning the phase diagram of Fig. 8. Then the zero bias anomaly follows all symmetry crossovers induced by experimentally tunable gate voltages and tunneling rates.

The main message of our work is that symmetry enters the realm of mesoscopic physics in a rather nontrivial manner. Dynamical symmetry in this context is not just a geometrical concept but, rather, intimately related with the physics of strong correlations and exchange interactions. The relation with other branches of physics makes it even more attractive. The groups $SO(n)$ play an important role in Particle Physics as well as in model building for high temperature superconductivity (especially $SO(5)$). The role of the group $SU(3)$ in Particle Physics cannot be overestimated and its role in Nuclear Physics in relation with the interacting Boson model is well recognized. This paper extends the role of these Lie groups in Condensed Matter Physics.

Acknowledgment: This work is partially supported by grants from the Israeli Science Foundations, the United States Israel Binational Science Foundation and Deutsche-Israeli-Project (DIP). One of us (T.K) is deeply indebted to the *Clore Scholars Programme* for generous support.

APPENDIX A: DIAGONALIZATION OF THE DOT HAMILTONIAN

Here we describe the diagonalization procedure of the Hamiltonian of the isolated TQDs occupied by four and three electrons. The dot Hamiltonian has the form,

$$H_d = \sum_{a=l,r,c}\sum_{\sigma}\epsilon_a d^\dagger_{a\sigma}d_{a\sigma} + \sum_a Q_a n_{a\uparrow}n_{a\downarrow} + \sum_{a=l,r}(W_a d^\dagger_{c\sigma}d_{a\sigma} + H.c.). \quad \text{(A1)}$$

(**a**) Four electron occupation:
The Hamiltonian (A1) can be diagonalized by using the basis of four-electron wave functions

$$|t_a,1\rangle = d^\dagger_{c\uparrow}d^\dagger_{a\uparrow}d^\dagger_{\bar{a}\uparrow}d^\dagger_{\bar{a}\downarrow}|0\rangle, \quad |t_a,\bar{1}\rangle = d^\dagger_{c\downarrow}d^\dagger_{a\downarrow}d^\dagger_{\bar{a}\uparrow}d^\dagger_{\bar{a}\downarrow}|0\rangle,$$
$$|t_a,0\rangle = \frac{1}{\sqrt{2}}\left(d^\dagger_{c\uparrow}d^\dagger_{a\downarrow} + d^\dagger_{c\downarrow}d^\dagger_{a\uparrow}\right)d^\dagger_{\bar{a}\uparrow}d^\dagger_{\bar{a}\downarrow}|0\rangle,$$
$$|s_a\rangle = \frac{1}{\sqrt{2}}\left(d^\dagger_{c\uparrow}d^\dagger_{a\downarrow} - d^\dagger_{c\downarrow}d^\dagger_{a\uparrow}\right)d^\dagger_{\bar{a}\uparrow}d^\dagger_{\bar{a}\downarrow}|0\rangle,$$
$$|ex\rangle = d^\dagger_{l\uparrow}d^\dagger_{l\downarrow}d^\dagger_{r\uparrow}d^\dagger_{r\downarrow}|0\rangle, \quad \text{(A2)}$$

where $a = l, r$; $\bar{l} = r$, $\bar{r} = l$. The Coulomb interaction quenches the states with two electrons in the central dot and we do not take them into account. The states (A2) form a basis of two triplet and three singlet states. In this basis, the Hamiltonian (A1) is decomposed into triplet and singlet matrices,

$$H_t = \begin{pmatrix} \tilde{\varepsilon}_l & 0 \\ 0 & \tilde{\varepsilon}_r \end{pmatrix}, \quad \text{(A3)}$$

and

$$H_s = \begin{pmatrix} \tilde{\varepsilon}_l & 0 & \sqrt{2}W_l \\ 0 & \tilde{\varepsilon}_r & \sqrt{2}W_r \\ \sqrt{2}W_l & \sqrt{2}W_r & \tilde{\varepsilon}_{ex} \end{pmatrix}, \quad \text{(A4)}$$

where $\tilde{\varepsilon}_l = \epsilon_c + \epsilon_l + 2\epsilon_r + Q_r$, $\tilde{\varepsilon}_r = \epsilon_c + \epsilon_r + 2\epsilon_l + Q_l$, and $\tilde{\varepsilon}_{ex} = 2\epsilon_l + 2\epsilon_r + Q_l + Q_r$. We are interested in the limit $\beta_a \ll 1$ (β_a are defined by Eq.(15)). So the secular

matrix may be diagonalized in lowest order of perturbation theory in β_a. The eigenfunctions corresponding to the energy levels (22) are

$$\begin{aligned}
&|S_a\rangle = \sqrt{1-2\beta_a^2}\,|s_a\rangle - \sqrt{2}\beta_a|ex\rangle,\\
&|T_a\rangle = |t_a\rangle\,,\\
&|Ex\rangle = \sqrt{1-2\beta_l^2-2\beta_r^2}\,|ex\rangle + \sqrt{2}\beta_l|s_l\rangle + \sqrt{2}\beta_r|s_r\rangle.
\end{aligned} \tag{A5}$$

In completely symmetric case, $\varepsilon_l = \varepsilon_r \equiv \varepsilon$, $Q_l = Q_r \equiv Q$, $W_l = W_r \equiv W$, the eigenfunctions corresponding to the energies (23) are

$$\begin{aligned}
|S_+\rangle &= \sqrt{1-4\beta^2}\frac{|s_l\rangle + |s_r\rangle}{\sqrt{2}} - 2\beta|ex\rangle,\\
|S_-\rangle &= \frac{|s_l\rangle - |s_r\rangle}{\sqrt{2}},\\
|T_\pm\rangle &= \frac{|t_l\rangle \pm |t_r\rangle}{\sqrt{2}},\\
|Ex\rangle &= \sqrt{1-4\beta}\,|ex\rangle + \sqrt{2}\beta(|s_l\rangle + |s_r\rangle),
\end{aligned} \tag{A6}$$

where $\beta = W/(\varepsilon + Q - \epsilon_c)$.

(**b**) Three electron occupation:

In this case the Hamiltonian (A1) can be diagonalized by using the basis of three–electron wave functions

$$\begin{aligned}
&|b,\sigma\rangle = \frac{([d^+_{c\uparrow}d^+_{l\downarrow} - d^+_{c\downarrow}d^+_{l\uparrow}]d^+_{r\sigma} + [d^+_{c\downarrow}d^+_{r\uparrow} - d^+_{c\uparrow}d^+_{r\downarrow}]d^+_{l\sigma})|0\rangle}{\sqrt{6}},\\
&|b_c,\sigma\rangle = -\frac{1}{\sqrt{2}}\left(d^+_{l\uparrow}d^+_{r\downarrow} - d^+_{l\downarrow}d^+_{r\uparrow}\right)d^+_{c\sigma}|0\rangle,\\
&\left|q,\pm\frac{3}{2}\right\rangle = d^+_{c\pm}d^+_{r\pm}d^+_{l\pm}|0\rangle,\\
&\left|q,\pm\frac{1}{2}\right\rangle = \frac{(d^+_{c\pm}d^+_{r\pm}d^+_{l\mp} + d^+_{c\pm}d^+_{r\mp}d^+_{l\pm} + d^+_{c\mp}d^+_{r\pm}d^+_{l\pm})|0\rangle}{\sqrt{3}},\\
&|b_{lc},\sigma\rangle = d^+_{l\uparrow}d^+_{l\downarrow}d^+_{c\sigma}|0\rangle, \qquad |b_{rc},\sigma\rangle = d^+_{r\uparrow}d^+_{r\downarrow}d^+_{c\sigma}|0\rangle,\\
&|b_l,\sigma\rangle = d^+_{r\uparrow}d^+_{r\downarrow}d^+_{l\sigma}|0\rangle, \qquad |b_r,\sigma\rangle = d^+_{l\uparrow}d^+_{l\downarrow}d^+_{r\sigma}|0\rangle,
\end{aligned} \tag{A7}$$

where $\sigma = \uparrow,\downarrow$. The three-electron states $|\Lambda\rangle$ of the TQD are classified as a ground state doublet $|B_1\rangle$, low-lying doublet $|B_2\rangle$ and quartet $|Q\rangle$ excitations, and four charge-transfer excitonic doublets B_{ac} and B_a $(a = l, r)$. In the framework of second order perturbation theory with respect to β_a (15), the energy levels E_Λ are

$$\begin{aligned}
E_{B_1} &= \epsilon_c + \epsilon_l + \epsilon_r - \frac{3}{2}\left[W_l\beta_l + W_r\beta_r\right],\\
E_{B_2} &= \epsilon_c + \epsilon_l + \epsilon_r - \frac{1}{2}\left[W_l\beta_l + W_r\beta_r\right],\\
E_Q &= \epsilon_c + \epsilon_l + \epsilon_r,\\
E_{B_{ac}} &= \epsilon_c + 2\epsilon_a + Q_a - W_{\bar a}\beta_{\bar a},\\
E_{B_a} &= \epsilon_a + 2\epsilon_{\bar a} + Q_{\bar a} + W_a\beta_a + 2W_{\bar a}\beta_{\bar a}.
\end{aligned} \tag{A8}$$

The eigenfunctions corresponding to the energy levels (A8) are the following combinations,

$$\begin{aligned}
&|B_1,\sigma\rangle = \gamma_1|b_1,\sigma\rangle - \frac{\sqrt{6}}{2}\beta_l|b_r,\sigma\rangle + \frac{\sqrt{6}}{2}\beta_r|b_l,\sigma\rangle,\\
&|B_2,\sigma\rangle = \gamma_2|b_2,\sigma\rangle - \frac{\sqrt{2}}{2}\beta_l|b_r,\sigma\rangle - \frac{\sqrt{2}}{2}\beta_r|b_l,\sigma\rangle,\\
&|Q,s_z\rangle = |q,s_z\rangle\,, \qquad s_z = \pm\frac{3}{2},\pm\frac{1}{2},\\
&|B_{ac},\sigma\rangle = \sqrt{1-\beta_{\bar a}^2}|b_{ac},\sigma\rangle - \beta_{\bar a}|b_{\bar a},\sigma\rangle,\\
&|B_r,\sigma\rangle = \sqrt{1-2\beta_l^2-\beta_r^2}|b_r,\sigma\rangle + \beta_r|b_{lc},\sigma\rangle\\
&\qquad + \frac{\sqrt{2}}{2}\beta_l\left(\sqrt{3}|b_1,\sigma\rangle + |b_2,\sigma\rangle\right),\\
&|B_l,\sigma\rangle = \sqrt{1-2\beta_r^2-\beta_l^2}|b_l,\sigma\rangle + \beta_l|b_r,c,\sigma\rangle\\
&\qquad - \frac{\sqrt{2}}{2}\beta_r\left(\sqrt{3}|b_1,\sigma\rangle - |b_2,\sigma\rangle\right),
\end{aligned} \tag{A9}$$

where γ_1 and γ_2 are determined by Eq.(79).

APPENDIX B: ROTATIONS IN THE SOURCE-DRAIN AND LEFT-RIGHT SPACE

In the generic case, the transformation which diagonalizes the tunneling Hamiltonian (25) has the form

$$\begin{pmatrix} c_{lek\sigma}\\ c_{lok\sigma}\\ c_{rek\sigma}\\ c_{rok\sigma}\end{pmatrix} = \begin{pmatrix} u_l & v_l & 0 & 0\\ -v_l & u_l & 0 & 0\\ 0 & 0 & u_r & v_r\\ 0 & 0 & -v_r & u_r\end{pmatrix}\begin{pmatrix} c_{lsk\sigma}\\ c_{ldk\sigma}\\ c_{rsk\sigma}\\ c_{rdk\sigma}\end{pmatrix} \tag{B1}$$

with $u_a = V_{as}/V_a$, $v_a = V_{ad}/V_a$; $V_a^2 = |V_{as}|^2 + |V_{ad}|^2$ $(a = l, r)$. In a symmetric case $V_{as} = V_{ad} = V$, this transformation simplifies to

$$\begin{aligned}
c_{aek\sigma} &= 2^{-1/2}\left(c_{ask\sigma} + c_{adk\sigma}\right),\\
c_{aok\sigma} &= 2^{-1/2}\left(-c_{ask\sigma} + c_{adk\sigma}\right),
\end{aligned} \tag{B2}$$

and only the even (e) combination survives in the tunneling Hamiltonian

$$H_{tun} = V\sum_{ak\sigma}(c^\dagger_{aek\sigma}d_{a\sigma} + H.c.). \tag{B3}$$

So the odd combination (o) may be omitted.

If, moreover, the whole system "TQD plus leads" possesses $l - r$ symmetry, $\varepsilon_l = \varepsilon_r$, the second rotation in $l - r$-space

$$\begin{pmatrix} c_{gk\sigma}\\ c_{uk\sigma}\\ d_{g\sigma}\\ d_{u\sigma}\end{pmatrix} = \frac{1}{\sqrt{2}}\begin{pmatrix} 1 & 1 & 0 & 0\\ -1 & 1 & 0 & 0\\ 0 & 0 & 1 & 1\\ 0 & 0 & -1 & 1\end{pmatrix}\begin{pmatrix} c_{lek\sigma}\\ c_{rek\sigma}\\ d_{l\sigma}\\ d_{r\sigma}\end{pmatrix} \tag{B4}$$

transforms $H_{lead} + H_{tun}$ into

$$H_{lead} + H_{tun} = \sum_{\eta k\sigma}\left[\epsilon_{k\eta}n_{\eta k\sigma} + V(c^\dagger_{\eta k\sigma}d_{\eta\sigma} + H.c.)\right] \tag{B5}$$

with $\epsilon_{kg} = \epsilon_k - t_{lr}$, $\epsilon_{ku} = \epsilon_k + t_{lr}$.

APPENDIX C: EFFECTIVE SPIN HAMILTONIAN

The spin Hamiltonian of the TQD with $N = 4$ occupation in series geometry (Fig.7) is derived below. The system is described by the Hamiltonian (67). The Schrieffer-Wolff transformation[27] for the configuration of four electron states of the TQD projects out three electron states $|\lambda\rangle$ and maps the Hamiltonian (67) onto an effective spin Hamiltonian $\widetilde{H}$ acting in a subspace of four-electron configurations $\langle\Lambda|\ldots|\Lambda'\rangle$,

$$\widetilde{H} = e^{i\mathcal{S}} H e^{-i\mathcal{S}} = H + \sum_m \frac{(i)^m}{m!}[\mathcal{S}, [\mathcal{S}...[\mathcal{S}, H]]...], \quad \text{(C1)}$$

where

$$\mathcal{S} = -i \sum_{\Lambda\lambda} \sum_{\langle k\rangle\sigma,a} \frac{V_{a\sigma}^{\Lambda\lambda}}{\bar{E}_{\Lambda\lambda} - \epsilon_{ka}} X^{\Lambda\lambda} c_{ak\sigma} + H.c. \quad \text{(C2)}$$

Here $\langle k\rangle$ stands for the electron or hole states whose energies are secluded within a layer $\pm\bar{D}$ around the Fermi level. $\bar{E}_{\Lambda\lambda} = E_\Lambda(\bar{D}) - E_\lambda(\bar{D})$ and the notation $a = l, r$ is used. The effective Hamiltonian with three–electron states $|\lambda\rangle$ frozen out can be obtained by retaining the terms to order $O(|V|^2)$ on the right-hand side of Eq.(C1). It has the following form,

$$\begin{aligned}\widetilde{H} \;=\; & \sum_\Lambda \bar{E}_\Lambda X^{\Lambda\Lambda} + \sum_{\langle k\rangle\sigma,a} \epsilon_{ka} c^+_{ak\sigma} c_{ak\sigma} \\ & - \sum_{\Lambda\Lambda'\lambda} \sum_{kk'\sigma\sigma'} \sum_{a=l,r} J^{\Lambda\Lambda'}_{kk'a} X^{\Lambda\Lambda'} c^+_{ak\sigma} c_{ak'\sigma'} \qquad \text{(C3)} \\ & - \sum_{\Lambda\Lambda'\lambda} \sum_{kk'\sigma\sigma'} (J^{\Lambda\Lambda'}_{kk'lr} X^{\Lambda\Lambda'} c^+_{rk\sigma} c_{lk'\sigma'} + H.c.),\end{aligned}$$

where

$$\begin{aligned} J^{\Lambda\Lambda'}_{kk'a} &= \frac{(V^{\lambda\Lambda}_{a\sigma})^* V^{\lambda\Lambda'}_{a\sigma'}}{2} \left(\frac{1}{\bar{E}_{\Lambda\lambda} - \epsilon_{ka}} + \frac{1}{\bar{E}_{\Lambda'\lambda} - \epsilon_{k'a}} \right), \\ J^{\Lambda\Lambda'}_{kk'lr} &= \frac{(V^{\lambda\Lambda}_{l\sigma})^* V^{\lambda\Lambda'}_{r\sigma'}}{2} \left(\frac{1}{\bar{E}_{\Lambda\lambda} - \epsilon_{kl}} + \frac{1}{\bar{E}_{\Lambda'\lambda} - \epsilon_{k'r}} \right) \quad \text{(C4)} \end{aligned}$$

The constraint $\sum_\Lambda X^{\Lambda\Lambda} = 1$ is valid. Unlike the conventional case of doublet spin 1/2 we have here an octet $\Lambda = \{\Lambda_l, \Lambda_r\} = \{S_l, T_l, S_r, T_r\}$, and the SW transformation *intermixes all these states*. The effective spin Hamiltonian (C3) to order $O(|V|^2)$ acquires the form of Eq.(68).

APPENDIX D: SO(7) SYMMETRY

The operators $\mathbf{S}_l$, $\mathbf{S}_r$, $\mathbf{R}_l$, $\tilde{\mathbf{R}}_1$, $\tilde{\mathbf{R}}_2$, $\tilde{\mathbf{R}}_3$ and A_i ($i = 1, 2, 3$) (see Eqs.(33),(63),(64)) obey the commutation relations of the o_7 Lie algebra,

$$\begin{aligned}
&[S_{aj}, S_{a'k}] = ie_{jkm}\delta_{aa'}S_{am}, \quad [R_{lj}, R_{lk}] = ie_{jkm}S_{lm},\\
&[R_{lj}, S_{lk}] = ie_{jkm}R_{lm}, \quad [R_{lj}, S_{rk}] = [\tilde{R}_{3j}, S_{lk}] = 0,\\
&[\tilde{R}_{3j}, \tilde{R}_{3k}] = ie_{jkm}S_{rm}, \quad [\tilde{R}_{3j}, S_{rk}] = ie_{jkm}\tilde{R}_{3m},\\
&[\tilde{R}_{1j}, \tilde{R}_{1k}] = ie_{jkm}S_{rm}(1-\delta_{jz})(1-\delta_{kz})\\
&\qquad +\frac{i}{2}e_{jkm}S_{lm}(\delta_{jz}+\delta_{kz}) - \frac{1}{2}(S_{lj}\delta_{kz} - S_{lk}\delta_{jz}),\\
&[\tilde{R}_{2j}, \tilde{R}_{2k}] = ie_{jkm}S_{lm}(1-\delta_{jz})(1-\delta_{kz})\\
&\qquad +\frac{i}{2}e_{jkm}S_{rm}(\delta_{jz}+\delta_{kz}) - \frac{1}{2}(S_{rj}\delta_{kz} - S_{rk}\delta_{jz}),\\
&[\tilde{R}_{1j}, \tilde{R}_{2k}] = \frac{i}{2}e_{jkm}(S_{rm}\delta_{jz} + S_{lm}\delta_{kz})\\
&\qquad +\frac{1}{2}\left[S_{lj}\delta_{kz} - S_{rk}\delta_{jz} + (S_{lz} - S_{rz})\delta_{jz}\delta_{kz}\right],\\
&[\tilde{R}_{3j}, \tilde{R}_{1k}] = ie_{jkm}R_{lm}(1-\delta_{jz} - \frac{\delta_{kz}}{2})\\
&\qquad -\frac{\delta_{kz}}{2}(1-\delta_{jz})R_{lj},\\
&[\tilde{R}_{3j}, \tilde{R}_{2k}] = ie_{jkm}R_{lm}(\delta_{jz} + \frac{\delta_{kz}}{2}) + \frac{\delta_{kz}}{2}(1-\delta_{jz})R_{lj},\\
&[\tilde{R}_{1j}, R_{lk}] = ie_{jkm}\tilde{R}_{3m}(\delta_{kz} + \frac{\delta_{jz}}{2}) - \frac{\delta_{jz}}{2}(1-\delta_{kz})\tilde{R}_{3k},\\
&[\tilde{R}_{2j}, R_{lk}] = ie_{jkm}\tilde{R}_{3m}(1-\delta_{kz} - \frac{\delta_{jz}}{2})\\
&\qquad +\frac{\delta_{jz}}{2}(1-\delta_{kz})\tilde{R}_{3k},
\end{aligned}$$

$$\begin{aligned}
&[A_1, S_{lj}] = iA_2\delta_{jz} + \frac{i\sqrt{2}}{2}(\tilde{R}_{1x}\delta_{jx} - \tilde{R}_{1y}\delta_{jy}),\\
&[A_2, S_{lj}] = -iA_1\delta_{jz} - \frac{i\sqrt{2}}{2}(\tilde{R}_{1y}\delta_{jx} + \tilde{R}_{1x}\delta_{jy}),\\
&[A_1, S_{rj}] = iA_2\delta_{jz} - \frac{i\sqrt{2}}{2}(\tilde{R}_{2x}\delta_{jx} - \tilde{R}_{2y}\delta_{jy}),\\
&[A_2, S_{rj}] = -iA_1\delta_{jz} + \frac{i\sqrt{2}}{2}(\tilde{R}_{2y}\delta_{jx} + \tilde{R}_{2x}\delta_{jy}),\\
&[A_3, S_{lj}] = -i\tilde{R}_{2j}(1-\delta_{jz}), \quad [A_3, S_{rj}] = i\tilde{R}_{1j}(1-\delta_{jz}),
\end{aligned}$$

$$
\begin{aligned}
&[A_1, R_{lj}] = -\frac{i\sqrt{2}}{2}(\tilde{R}_{3x}\delta_{jx} - \tilde{R}_{3y}\delta_{jy}),\\
&[A_2, R_{lj}] = \frac{i\sqrt{2}}{2}(\tilde{R}_{3y}\delta_{jx} + \tilde{R}_{3x}\delta_{jy}),\\
&[A_1, \tilde{R}_{3j}] = \frac{i\sqrt{2}}{2}(R_{lx}\delta_{jx} - R_{ly}\delta_{jy}),\\
&[A_2, \tilde{R}_{3j}] = -\frac{i\sqrt{2}}{2}(R_{ly}\delta_{jx} + R_{lx}\delta_{jy}),\\
&[A_3, R_{lj}] = -i\tilde{R}_{3z}\delta_{jz}, \qquad [A_3, \tilde{R}_{3j}] = iR_{lz}\delta_{jz},\\
&[A_1, \tilde{R}_{1j}] = -\frac{i\sqrt{2}}{2}(S_{lx}\delta_{jx} - S_{ly}\delta_{jy}),\\
&[A_2, \tilde{R}_{1j}] = \frac{i\sqrt{2}}{2}(S_{ly}\delta_{jx} + S_{lx}\delta_{jy}),\\
&[A_3, \tilde{R}_{1j}] = -i(S_{rx}\delta_{jx} + S_{ry}\delta_{jy}),\\
&[A_1, \tilde{R}_{2j}] = \frac{i\sqrt{2}}{2}(S_{rx}\delta_{jx} - S_{ry}\delta_{jy}),\\
&[A_2, \tilde{R}_{2j}] = -\frac{i\sqrt{2}}{2}(S_{ry}\delta_{jx} + S_{rx}\delta_{jy}),\\
&[A_3, \tilde{R}_{2j}] = i(S_{lx}\delta_{jx} + S_{ly}\delta_{jy}),\\
&[A_1, A_2] = -i(S_{lz} + S_{rz}), \qquad [A_1, A_3] = [A_2, A_3] = 0,\\
&[S_{aj}, \tilde{R}_{\mu k}] = \tau^{a\mu\nu}_{jkm}\tilde{R}_{\mu m} + \alpha^{a\mu n}_{jk}A_n,\\
&[\tilde{R}_{3j}, R_{lk}] = \beta^{\mu}_{jkm}\tilde{R}_{\mu m} + \tilde{\alpha}^{n}_{jk}A_n. \qquad \text{(D1)}
\end{aligned}
$$

Here j, k, m are Cartesian indices, $a = l, r$; $\mu, \nu = 1, 2$; $n = 1, 2, 3$; $\tau^{a\mu\nu}_{jkm}$, $\alpha^{a\mu n}_{jk}$, $\tilde{\alpha}^{n}_{jk}$ and β^{μ}_{jkm} are the structural constants, $\tau^{l\mu\nu}_{jkm} = \tau^{r\bar{\mu}\bar{\nu}}_{jkm}$, $\alpha^{l\mu n}_{jk} = -\alpha^{r\bar{\mu}n}_{jk}$ ($\bar{1} = 2$, $\bar{2} = 1$). Their non-zero components are:

$$
\begin{aligned}
\tau^{l11}_{xxz} &= \tau^{l11}_{xzx} = \tau^{l11}_{yyz} = \tau^{l11}_{yzy} = \frac{1}{2},\\
\tau^{l21}_{xzx} &= \tau^{l21}_{yzy} = \tau^{l12}_{xxz} = \tau^{l12}_{yyz} = -\frac{1}{2},\\
\tau^{l11}_{xyz} &= \tau^{l12}_{xyz} = \tau^{l21}_{yzx} = \frac{i}{2},\\
\tau^{l11}_{xzy} &= \tau^{l11}_{yxz} = \tau^{l12}_{yxz} = \tau^{l21}_{xzy} = -\frac{i}{2},\\
\tau^{l11}_{zzz} &= 1,\ \tau^{l22}_{zzz} = -1,\ \tau^{l22}_{zxy} = i,\ \tau^{l22}_{zyx} = -i,
\end{aligned}
$$

$$
\begin{aligned}
\alpha^{l11}_{xy} &= \alpha^{l11}_{yx} = \frac{\sqrt{2}}{2}, \quad \alpha^{l12}_{xy} = \alpha^{l12}_{yx} = -\frac{\sqrt{2}}{2},\\
\alpha^{l11}_{xx} &= \alpha^{l12}_{xx} = \frac{i\sqrt{2}}{2}, \quad \alpha^{l11}_{yy} = \alpha^{l12}_{yy} = -\frac{i\sqrt{2}}{2},\\
\alpha^{l23}_{xx} &= \alpha^{l23}_{yy} = -i\sqrt{2},
\end{aligned}
$$

$$
\begin{aligned}
\beta^{1}_{xxz} &= \beta^{2}_{yyz} = -\frac{1}{2}, \quad \beta^{2}_{xxz} = \beta^{1}_{yyz} = \frac{1}{2},\\
\beta^{1}_{xyz} &= \beta^{2}_{xyz} = \frac{i}{2}, \quad \beta^{1}_{yxz} = \beta^{2}_{yxz} = -\frac{i}{2},\\
\beta^{1}_{xzy} &= \beta^{2}_{zyx} = -i, \quad \beta^{1}_{yzx} = \beta^{2}_{zxy} = i,
\end{aligned}
$$

$$
\tilde{\alpha}^{1}_{xx} = \tilde{\alpha}^{3}_{zz} = i\sqrt{2}, \quad \tilde{\alpha}^{2}_{xy} = \tilde{\alpha}^{2}_{yx} = \tilde{\alpha}^{1}_{yy} = -i\sqrt{2}.
$$

The following relations hold,

$$
\begin{aligned}
&\mathbf{S}_a \cdot \mathbf{R}_l = \mathbf{S}_a \cdot \tilde{\mathbf{R}}_3 = 0, \quad A_1A_3 = A_2A_3 = 0,\\
&\mathbf{S}_a^2 = 2X^{\mu_a\mu_a},\ \tilde{\mathbf{R}}_1 \cdot \tilde{\mathbf{R}}_1^{\dagger} + \tilde{\mathbf{R}}_2 \cdot \tilde{\mathbf{R}}_2^{\dagger} = 2\sum_{a=l,r} X^{\mu_a\mu_a},\\
&\mathbf{R}_l^2 = X^{\mu_l\mu_l} + 3X^{S_lS_l}, \quad \tilde{\mathbf{R}}_3^2 = X^{\mu_r\mu_r} + 3X^{S_lS_l},\\
&A_1^2 + A_2^2 + A_3^2 = X^{\mu_l\mu_l} + X^{\mu_r\mu_r}. \qquad \text{(D2)}
\end{aligned}
$$

Therefore, the vector operators $\mathbf{S}_l$, $\mathbf{S}_r$, $\mathbf{R}_l$, $\tilde{\mathbf{R}}_i$ and scalar operators A_i ($i = 1, 2, 3$) generate the algebra o_7 in a representation specified by the Casimir operator

$$
\mathbf{S}_l^2 + \mathbf{S}_r^2 + \mathbf{R}_l^2 + \sum_{i=1}^{2} \tilde{\mathbf{R}}_i \cdot \tilde{\mathbf{R}}_i^{\dagger} + \tilde{\mathbf{R}}_3^2 + \sum_{i=1}^{3} A_i^2 = 6. \quad \text{(D3)}
$$

APPENDIX E: YOUNG TABLEAUX CORRESPONDING TO VARIOUS SYMMETRIES

A TQD with "passive" central dot and "active" side dots reminds an artificial atom with inner core and external valence shell. The many-electron wave functions in this nanoobject may be symmetrized in various ways, so that each spin state of N electrons in the TQD is characterized by its own symmetrization scheme. One may illustrate these schemes by means of the conventional graphic presentation of the permutation symmetry of multi-electron system by Young tableau[36]. For instance, triplet state of two electrons which is symmetric with respect to the electron permutation is labeled by a row of two squares, whereas the singlet one which is antisymmetric with respect to the permutation is labeled by a column of two squares. Having this in mind we can represent the singlet and triplet four electron states of the TQD (A5) by the four tableaux shown in Fig.11. The tableaux S_l (S_r) and T_l (T_r) correspond to the singlet and triplet states in which the right (left) dot contains two electrons (grey column in Fig.11) whereas electrons in the left (right) and central dots form singlet and triplet, respectively.

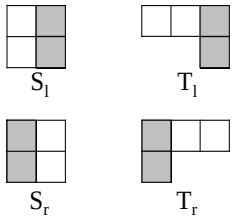

FIG. 11: Young tableaux corresponding to the singlet (S_a) and triplet (T_a) four electron states of the TQD. The grey column denote two electrons in the same dot (right or left).

The Young tableaux corresponding to various $SO(n)$ symmetries discussed in Sec.III can be obtained by combining the appropriate tableaux (Fig. 12). The highest possible symmetry $P \times SO(4) \times SO(4)$ is represented

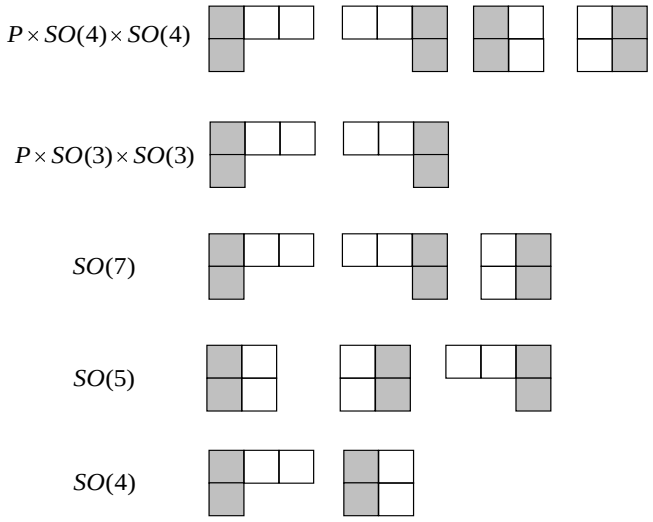

FIG. 12: Young tableaux corresponding to $SO(n)$ symmetries.

by four tableaux T_l, T_r, S_l and S_r since all singlet and triplet states are degenerate in this case. The symmetry $P\times SO(3)\times SO(3)$ occurs when two triplets T_l and T_r are close in energy and these are represented by the couple of Young tableaux in the second line. Following this procedure, the $SO(7)$ symmetry can be described in terms of two triplets T_l, T_r diagrams and one singlet S_l diagram. Moreover, $SO(5)$ symmetry is represented by two singlet S_l, S_r diagrams and one triplet T_l diagram and, finally, one triplet and one singlet tableaux correspond to the $SO(4)$ symmetry.

[1] *Atomic and Molecular Wires*, edited by C. Joachim and S. Roth (Kluwer, Dordrecht, 1996); L.P. Kouwenhoven, D.G. Austing and S. Tarucha, Rep. Progr. Phys. **64**, 701 (2001).

[2] *Nanophysics and Bio-Electronics*, edited by T. Chakraborty, F. Peeters, and U. Sivan (Elsevier, Amsterdam, 2002).

[3] F. Guinea and G. Zimanyi, Phys. Rev. B **47**, 501 (1993); R. Mukhopadhyay, C.L. Kane, and T. C. Lubensky, Phys. Rev. B **63**, 081103 (2001); I. Kuzmenko, S. Gredeskul, K. Kikoin, and Y. Avishai, Phys. Rev. B **67**, 115331 (2003).

[4] B.J. van Wees, H. van Houten, C.W.J. Beenakker, J.G. Williamson, L.P. Kouwenhoven, D. van der Marel, and C.T. Foxon, Phys. Rev. Lett. **60**, 848 (1988); K.J. Thomas, J.T. Nicholls, N.J. Appleyard, M.Y. Simmons, M. Pepper, D.R. Mace, W.R. Tribe, and D.A. Ritchie, Phys. Rev. B **58**, 4846 (1998).

[5] S. Hershfield, J.H. Davies, and J.W. Wilkins, Phys. Rev. Lett. **67**, 3720 (1991); Y. Meir, N.S. Wingreen, and P.A. Lee, Phys. Rev. Lett. **70**, 2601 (1993); M.H. Hettler, J. Kroha, and S. Hershfield, Phys. Rev. B **58**, 5649 (1998).

[6] M. Pustilnik, Y. Avishai, and K. Kikoin, Phys. Rev. Lett. **84**, 1756 (2000); M. Eto and Yu. Nazarov, Phys. Rev. Lett. **85**, 1306 (2000); D. Guiliano and F. Tagliacozzo, Phys. Rev. B **63**, 125318 (2001).

[7] Y. Goldin and Y. Avishai, Phys. Rev. Lett. **81**, 5394 (1998), Phys. Rev. B **61**, 16750 (2000); K. Kikoin, M. Pustilnik, and Y. Avishai, Physica B **259-261,** 217 (1999); K.A. Kikoin and Y. Avishai, Phys. Rev. B **62**, 4647 (2000); T.V. Shahbazyan, I.E. Perakis, and M.E. Raikh, Phys. Rev. Lett. **84**, 5896 (2000); T. Fujii and N. Kawakami, Phys. Rev. B **63**, 054414 (2001).

[8] A. Yacobi, M. Heiblum, D. Mahalu, and H. Shtrikman, Phys. Rev. Lett. **74**, 4047 (1995); Y. Li, M. Heiblum, and H. Strikman, Phys. Rev. Lett. **88**, 076601 (2002); U. Gerland, J. von Delft, T.A. Costi, and Y. Oreg, Phys. Rev. Lett. **84**, 3710 (2000).

[9] D. Goldhaber-Gordon, H. Shtrikman, D. Mahalu, D. Abush-Magder, U. Meirav, and M.A. Kastner, Nature **391**, 156 (1998); S.M. Cronenwett, T.H. Oosterkamp, and L.P. Kouwenhoven, Science **281**, 540 (1998).

[10] G.A. Fiete, J.S. Hersch, and E.J. Heller, Phys. Rev. Lett. **86**, 2392 (2001); M.A. Schneider, Phys. Rev. B **65**, 121406 (2002); J. Park, A.N. Pasupathy, J.I. Goldsmith, C. Chang, Y. Yaish, J.R. Petta, M. Rinkoski, J.P. Sethna, H.D. Abruna, P.L. Mceuen, and D.C. Ralph, Nature **417**, 722 (2002); W. Liang, M.P. Shores, M. Bockrath, J.R. Long, and H. Park, Nature **417**, 725 (2002).

[11] L. Glazman and M. Raikh, JETP Lett. **47**, 452 (1988); T.-K. Ng and P. A. Lee, Phys. Rev. Lett., **61**, 1768 (1988).

[12] K. Kikoin and Y. Avishai, Phys. Rev. Lett. **86**, 2090 (2001).

[13] K. Kikoin and Y. Avishai, Phys. Rev. B **65**, 115329 (2002).

[14] T. Kuzmenko, K. Kikoin and Y. Avishai, Phys. Rev. Lett. **89**, 156602 (2002).

[15] M.J. Englefield, *Group Theory and the Coulomb Problem* (Wiley, New York, 1972); I.A. Malkin and V.I. Man'ko, *Dynamical Symmetries and Coherent States of Quantum Systems* (Fizmatgiz, Moscow 1979).

[16] J. Hubbard, Proc. Roy. Soc. A **285**, 542 (1965); see also Yu.P. Irkhin, Sov. Phys. - JETP **50**, 379 (1966).

[17] The Coulomb potential possesses occasional degeneracy of the states with different moments **l**. So, according to (3) the Runge-Lenz vector is the integral of motion. In this case one speaks about *hidden* symmetry of the system.

[18] Y. Dothan, M. Gell-Mann and Y. Neeman, Phys. Lett. **17**, 148 (1965).

[19] P. W. Anderson, J. Phys. C.: Solid. St. Phys., **3**, 2435 (1970).

[20] F. D. M. Haldane Phys. Rev. Lett. **40**, 416 (1978).

[21] M. Pustilnik and L.I. Glazman, Phys. Rev. B **64**, 045328 (2001).

[22] M. Eto and Yu. Nazarov, Phys. Rev. B **66**, 153319 (2002).

[23] A. de-Shalit and I. Talmi, *Nuclear Shell Theory*, Academic Press, New York and London (1963).

[24] R.N. Cahn, *Semi-Simple Lie Algebras and their representations* (Benjamin, 1984).

[25] J. Nygård, D.H. Cobden and P.E. Lindelof, Nature **408**, 342 (2000); N S. Sasaki, S. De Franceschi, J.M. Elzermann, *et al.,* Nature, **405**, 764 (2000).
[26] A.C. Hewson, *The Kondo problem to Heavy Fermions* (Cambridge University Press, 1997).
[27] J.R. Schrieffer and P.A. Wolff, Phys. Rev. **149**, 491 (1966).
[28] T. Kuzmenko, K. Kikoin and Y. Avishai, Europhys. Lett. **64**, 218 (2003).
[29] K. Kang, S.Y. Cho, J-J. Kim, and S-C. Shin, Phys. Rev. B **63**, 113304 (2001); T-S. Kim and S. Hershfield, Phys. Rev. B **63**, 245326 (2001); Y. Takazawa, Y. Imai, and N. Kawakami, J. Phys. Soc. Jpn, **71**, 2234 (2002).
[30] P. Nozieres and A. Blandin, J. Phys. (Paris) **41**, 193 (1980).
[31] P.W. Anderson, G. Yuval and D.R. Hamann, Phys. Rev. B**1**, 4464 (1970); H. Shiba, Progr. Theor. Phys. **43**, 601 (1970).
[32] D.L. Cox and A. Zawadowski, Adv. Phys. **47**, 599 (1998).
[33] I.S. Sandalov and A.N. Podmarkov, Sov. Phys. JETP **61**, 783 (1985).
[34] F.P. Onufrieva, Sov. Phys. JETP **53**, 1241 (1981) [JETP **80**, 2372 (1981)]; Sov. Phys. JETP **59**, 986 (1984) [JETP **86**, 1691 (1984)].
[35] L-A. Wu, M. Guidry, Y. Sun and C-L. Wu, Phys. Rev. B **67**, 014515 (2003).
[36] J.P. Elliot and P.G. Dawber, *Symmetry in Physics* (Oxford University Press, 1984).